



KARADENİZ TECHNICAL UNIVERSITY
THE GRADUATE SCHOOL OF NATURAL AND APPLIED SCIENCES
DEPARTMENT OF ELECTRICAL AND ELECTRONICS ENGINEERING

**DESIGN AND SIMULATION OF SINGLE, DOUBLE, AND MULTI-LAYER
ANTIREFLECTION COATING FOR CRYSTALLINE SILICON SOLAR CELL**

Al-Montazer MANDONG

**This thesis is accepted to give the degree of
"MASTER OF SCIENCE"**

**By
The Graduate School of Natural and Applied Sciences at
Karadeniz Technical University**

The Date of Submission : 03 /01 /2019

The Date of Examination : 21 /01 /2019

Supervisor : Dr. Öğr. Üyesi Abdullah ÜZÜM

Trabzon 2019

KARADENİZ TECHNICAL UNIVERSITY
THE GRADUATE SCHOOL OF NATURAL AND APPLIED SCIENCES

Department of Electrical and Electronics Engineering
AI-Montazer MANDONG

**DESIGN AND SIMULATION OF SINGLE, DOUBLE, AND MULTI-LAYER
ANTIREFLECTION COATING FOR CRYSTALLINE SILICON SOLAR CELL**

Has been accepted as a thesis of
MASTER OF SCIENCE
after the Examination by the Jury Assigned by the Administrative Board of
the Graduate School of Natural and Applied Sciences with the Decision Number1785 dated
03 /01 / 2019

Approved By

Chairman : Doç. Dr. Kadir TÜRK

Member : Doç. Dr. Yunus AKALTUN

Member : Dr. Öğr. Üyesi Abdullah ÜZÜM

Prof. Dr. Sadettin KORKMAZ
Director of Graduate School

PREFACE

This work was done at Department of Electrical and Electronics Engineering at Karadeniz Technical University, Trabzon Turkey.

Firstly, I would like to thank my parents JANIA and JENIEH MANDONG who have taught, supported and guided me throughout my life. I would never become who I am today without their support.

I would also like to thank my supervisor Dr. Öğr. Üyesi Abdullah ÜZÜM for accepting and guiding me throughout my work. I admire his knowledge, experience and expertise in the field of photovoltaic systems which helped me substantially during the period of my work.

Also, I would like to thank all the people who became part of my academic life specially the professors of Department of Electrical and Electronics Engineering for imparting their knowledge and insights in their own fields of expertise.

Lastly, I would also like to thank my relatives, colleagues, my wife Karina Azzahra and son for always becoming my source of strength and inspiration.

Al Montazer MANDONG
Trabzon 2019

DECLARATION

I declare that this thesis entitled ‘Design and Simulation of Single, Double and Multi-layered Antireflection Coating for Crystalline Silicon Solar Cells’ is an original research. It is written by me and has not been submitted to any previous university or published in any institution. I confirm that the work submitted is my own work, except for the different data and information from other publications which has been cited in the reference section. My own contribution and that of the other authors have been properly indicated and cited in this work. 21/01/2019.



Al Montazer MANDONG

TABLE OF CONTENTS

| | <u>Page No.</u> |
|-------------------------------------------------------------|-----------------|
| PREFACE | III |
| DECLARATION | IV |
| TABLE OF CONTENTS | V |
| ÖZET | VII |
| SUMMARY | VIII |
| LIST OF FIGURES | IX |
| LIST OF TABLES | XI |
| LIST OF ACRONYMS AND ABBREVIATION | XII |
| LIST OF SYMBOLS | XIII |
| 1. INTRODUCTION | 1 |
| 1.1. Thesis Objectives | 1 |
| 1.2. Purpose of the Study | 2 |
| 1.3. Thesis Outline | 3 |
| 1.4. World Energy Consumption | 3 |
| 1.5. Importance of Renewable Energy | 4 |
| 1.6. Renewable Energy Usage | 4 |
| 1.7. Solar Cell Efficiencies | 6 |
| 1.8. Types of Solar Cells | 7 |
| 1.9. Crystalline Silicon (c-Si) Solar Cells | 8 |
| 2. WORKING PRINCIPLES OF CRYSTALLINE SILICON SOLAR CELLS .. | 9 |
| 2.1. Structure of c-Si Solar Cells | 9 |
| 2.2. Properties of Light | 10 |
| 2.3. Photon Flux | 10 |
| 2.4. Spectral Irradiance | 11 |
| 2.5. Band Gap | 12 |
| 2.6. Transport Mechanisms | 13 |
| 2.6.1. Diffusion | 13 |
| 2.6.2. Drift | 14 |
| 2.7. Recombination | 15 |
| 2.8. PN Junction | 15 |

| | | |
|--------|------------------------------------------------------|----|
| 2.8.1. | PN Junction Without Illumination | 16 |
| 2.8.2. | PN Junction Under Illumination | 17 |
| 2.9. | Solar Cell Performance | 18 |
| 2.9.1. | Short Circuit Current..... | 19 |
| 2.9.2. | Open Circuit Voltage | 19 |
| 2.9.3. | I-V Curve | 20 |
| 2.9.4. | Fill Factor | 21 |
| 2.9.5. | Efficiency | 21 |
| 3. | WORKING PRINCIPLES OF ANTI-REFLECTION COATING | 22 |
| 3.1. | Wave Nature of Light | 22 |
| 3.2. | Particle Nature of Light..... | 23 |
| 3.3. | Wave Superposition | 23 |
| 3.4. | Interaction of Waves With Other Materials | 24 |
| 3.5. | Absorption of Light..... | 25 |
| 3.6. | Refraction..... | 26 |
| 3.7. | Refractive Index | 26 |
| 3.8. | Reflection..... | 27 |
| 3.9. | Polarization | 28 |
| 3.10. | Fresnel's Equations | 29 |
| 4. | SIMULATION OF ANTI-REFLECTION COATING | 30 |
| 4.1. | Single Layer Anti-Reflection Coating | 31 |
| 4.1.1. | Comparison of Experimental and Simulated SLARC | 34 |
| 4.2. | Double Layer Anti-Reflection Coating (DLARC)..... | 36 |
| 4.2.1. | Comparison of Measured and Simulated DLARC | 38 |
| 4.3. | Multi Layer Anti-Reflection Coating (MLARC)..... | 39 |
| 4.3.1. | Simulation of Alternative MLARCs | 40 |
| 4.4. | PC1D Simulations..... | 41 |
| 5. | CONCLUSIONS AND RECOMMENDATIONS | 43 |
| 6. | REFERENCES..... | 44 |

CURRICULUM VITAE

Yüksek Lisans Tezi

ÖZET

KRİSTAL SİLİSYUM GÜNEŞ HÜCRELERİ İÇİN TEK, ÇİFT VE ÇOK KATMANLI
YANSIMAYI ÖNLEYİCİ TABAKALARIN TASARIMI VE SİMÜLASYONU

Al Montazer MANDONG

Karadeniz Teknik Üniversitesi
Fen Bilimleri Enstitüsü
Elektrik-Elektronik Mühendisliği Anabilim Dalı
Danışman: Dr. Öğr. Üyesi Abdullah ÜZÜM
2019, 49 Sayfa

Güneş hücrelerinin yüzeylerine gelen fotonların bir kısmı dalga boylarına göre yansır, bir kısmı emilir veya hücre içerisinden emilemeden geçerler. Yansıyan ve soğurulamayan fotonlar optiksel kayıp olarak sonuçlanacaktır. Dolayısıyla taşıyıcı oluşumuna katkı sağlayamadıkları için hücre veriminin düşmesine neden olmaktadır. Bu nedenle, güneş hücrelerinde hücre yüzeyine gelen fotonların maksimum seviyede soğurulması ve bu sayede taşıyıcı oluşumuna katkı sağlayarak yüksek verim elde edilebilmesi için çok önemlidir. Yansımayı önleyici yöntemlerden bazıları standart olarak kullanılan yüzey pürüzleştirme ve yansımayı önleyici ince film uygulamalarıdır. Özellikle yansımayı önleyici ince filmler kullanılarak optiksel soğurmayı arttırarak yansımayı önlemek ve hücre verimini arttırmak yüksek verimlere ulaşabilmek için son derece gereklidir. Yüksek verimli hücreler için en uygun malzemenin ve parametrelerin belirlenmesi ve bu tür ince filmlerin güneş hücrelerine uygulanmasını simülasyon çalışmalarıyla ortaya koyabilmek önemlidir. Bu çalışmada kristal silisyum güneş hücreleri için yansımayı önleyici tabakaların çalışma prensipleri, matematiksel olarak parametrelerinin belirlenmesi ve simülasyon çalışmaları farklı yöntemler kullanılarak hesaplanmış ve deneysel verilerle karşılaştırılmıştır. Tek, çift ve çok katmanlı yansımayı önleyici ince filmler için matematiksel çalışmalar MATLAB programı ile her yöntem için ayrı ayrı ele alınmış ve deneysel ölçümlerle karşılaştırılarak doğrulukları teyit edilmiştir. Ayrıca, PC1D simülasyon programı yardımıyla matematiksel olarak belirlenmiş optimal değerlerle güneş hücreleri simülasyonları gerçekleştirilmiştir.

Anahtar Kelimeler: *yansımayı önleyici tabaka, güneş hücreleri, yarıiletken aygıtlar, ince filmler, simülasyon*

Master Thesis

SUMMARY

DESIGN AND SIMULATION OF SINGLE, DOUBLE, AND MULTI-LAYER
ANTIREFLECTION COATING FOR CRYSTALLINE SILICON SOLAR CELL

Al Montazer MANDONG

Karadeniz Technical University
Graduate School of Natural and Applied Sciences
Electrical and Electronics Engineering Graduate Program
Supervisor: Asst. Prof. Abdullah ÜZÜM
2019, 49 Pages

Efficient absorption of light into the device is of utmost importance in the design of an efficient solar cells. A portion of incident light is reflected due to inherent reflectance of the materials used in fabricating the solar cell. These reflections can significantly reduce the generation of charge carriers which results to lower efficiency. One of the most important technique that became an integral part of modern solar cells today in order achieve maximum efficiency is the antireflection coating layer. Antireflection coating is a thin layer of dielectric material deposited on the silicon substrate in order to reduce the optical losses due to reflection and increase the transmittance of light, thus improving the solar cell's overall efficiency. An accurate computer simulation based on fundamentals of light and thin films are needed in order to select the best design of antireflection coating layers for the optimum performance of the solar cell. This study aims to understand the fundamental working principles and the mathematical equations of thin films that are used as antireflection coatings on crystalline silicon solar cells. Mathematical equations for single, dual and multi-layered ARC are presented and simulated with the use of MATLAB. Various experimental measurements were used to validate the accuracy of the mathematical equations that are used in this study. In addition, PC1D simulations are also used for validating the reflectance spectra and measuring the performance of solar cells with different combinations of antireflection coating.

Key Words: *antireflection coating, solar cell, semiconductor device, thin films, simulation*

LIST OF FIGURES

| | <u>Page No.</u> |
|----------------------------------------------------------------------------|-----------------|
| Figure 1. Global energy expenditure by source and scenario | 4 |
| Figure 2. Global renewable energy capacity in MW from 2007 to 2016 | 5 |
| Figure 3. Global average annual capacity additions from 2017 to 2040 | 5 |
| Figure 4. Solar cell efficiency timeline | 6 |
| Figure 5. Monocrystalline and polycrystalline silicon wafers | 8 |
| Figure 6. Basic structure of a crystalline silicon solar cell | 9 |
| Figure 7. The Electromagnetic spectrum | 10 |
| Figure 8. Photon flux based on AM 1.5G spectrum | 11 |
| Figure 9. AM 1.5G global spectrum | 11 |
| Figure 10. Excitation process from valence to conduction band | 12 |
| Figure 11. Diffusion of carriers | 13 |
| Figure 12. Drift mechanism | 14 |
| Figure 13. Working principle of PN junction solar cells | 16 |
| Figure 14. P-N junction without illumination | 17 |
| Figure 15. P-N junction under illumination | 18 |
| Figure 16. Equivalent circuit of solar cells | 18 |
| Figure 17. Solar cell IV curve | 20 |
| Figure 18. Characteristics of a wave | 22 |
| Figure 19. Types of photons and their wavelengths | 23 |
| Figure 20. Wave superposition | 24 |
| Figure 21. Absorption coefficients of semiconductor materials | 25 |
| Figure 22. Snell's law | 26 |
| Figure 23. Refractive index of common dielectric materials | 27 |
| Figure 24. Reflection of waves between two different mediums | 27 |
| Figure 25. Reflection of polarized and unpolarized light on silicon | 28 |
| Figure 26. Fresnel reflections | 29 |
| Figure 27. Reflections in solar cells | 30 |
| Figure 28. Constructive and destructive interference | 31 |
| Figure 29. Single layer anti-reflection coating | 32 |

| | |
|-----------------------------------------------------------------------------------------|----|
| Figure 30a. Uncoated Si solar cell | 35 |
| Figure 30b. Solar cell with TiO_2 ARC | 35 |
| Figure 30c. Solar cell with Ta_2O_5 ARC | 35 |
| Figure 30d. Solar cell with SiN_x ARC | 35 |
| Figure 31. Interacting waves within double layer anti-reflection coating | 36 |
| Figure 32a. Solar cell with $\text{TiO}_2/\text{SiN}_x$ ARC | 38 |
| Figure 32b. Solar cell with MgF_2/ZnS ARC | 38 |
| Figure 33. Interacting waves within solar cell with MLARC..... | 39 |
| Figure 33a. Solar cell with $\text{SiO}_2/\text{Al}_2\text{O}_3/\text{TiO}_2$ ARC | 40 |
| Figure 33b. Solar cell with $\text{MgF}_2/\text{SiO}_2/\text{TiO}_2$ ARC | 40 |

LIST OF TABLES

| | <u>Page No.</u> |
|--------------------------------------------------------------------------------------|------------------------|
| Table 1. Average reflectance of solar cells with SLARC using different methods | 35 |
| Table 2. Average reflectance of solar cells with DLARC using different methods | 38 |
| Table 3. Average reflectance of solar cells with MLARC using different methods | 40 |
| Table 4. Solar cell device parameters using PC1D | 41 |
| Table 5. Device performance of Solar Cells with different ARC | 42 |



LIST OF ACRONYMS AND ABBREVIATION

Al₂O₃ – Aluminum Oxide
ARC – Anti Reflection Coating
CdTe – Cadmium Telluride
CIGS – Copper Indium Gallium Selenide Solar Cell
DLARC – Double Layer Anti Reflection Coating
EM – Electromagnetic
FF – Fill Factor
GaAs – Gallium Arsenide
HfO₂ – Hafnium dioxide
IEA – International Energy Agency
InAs – Indium Arsenide
IRENA – International Renewable Energy Agency
MgF₂ – Magnesium Fluoride
MPP – Maximum Power Point
MW – Megawatts
NPS – New policy Scenario
NREL – National Renewable Energy Laboratory
PECVD – Plasma-Enhanced Chemical Vapor Deposition
PV – Photovoltaic
SDS – Sustainable Development Scenario
SiN_x – Silicon Nitride
SiO₂ – Silicon Dioxide
SLARC – Single Layer Anti Reflection Coating
SRH – Shockley-Read-Hall
Ta₂O₅ – Tantalum Pentoxide
TiO₂ – Titanium Dioxide
ZnS – Zinc Sulfide
ZrO₂ – Zirconium Dioxide

LIST OF SYMBOLS

c = speed of light

d = thickness of the ARC in nm

d_1 = thickness of 1st layer ARC in nm

d_2 = thickness of 2nd layer ARC in nm

eV = electron volts

f = frequency

FF – Fill Factor

h = planck's constant

I_d – diode current

I_{dark} – Dark Current

I_{mp} – Current at maximum powerpoint

I_o – Reverse saturation current

I_{ph} – Current generated by photons

I_{sc} – Short-circuit current

J_{sc} – Short-circuit current density

k – Boltzmann's Constant

k_1 = extinction coefficient of ARC

k_2 = extinction coefficient of substrate

n = refractive index

n_o = refractive index of air

n_1 = refractive index of substrate

n_i = refractive index of incident medium

n_t = refractive index of 2nd medium

P_{in} = input power

P_{max} – Maximum power

q – electric charge

R = total reflection

r_p = p-polarized reflectance coefficient

R_s – Parasitic series resistance

R_{sh} – Parasitic shunt resistance

r_l = reflection coefficient of ARC

r_{01} = reflectance at interface 0 to 1

r_{10} = reflectance at interface 1 to 0

r_{12} = reflectance at interface 1 to 2

r_s = s-polarized reflectance coefficient

T – Temperature in kelvin

t_s = s-polarized transmission coefficient

t_p = p-polarized reflectance coefficient

t_{01} = transmittance at interface 0 to 1

t_{10} = transmittance at interface 1 to 0

V – Voltage across the diode

V_{mp} – Voltage at maximum power point

V_{oc} – Open Circuit voltage

V_p = velocity of propagation at medium p

η = efficiency

λ = wavelength

λ_p = wavelength of propagation at medium p

θ_i = angle of incidence

θ_t = angle of transmission

λ_o = wavelength in free space

1. INTRODUCTION

Conventional sources of energy such as gasoline, diesel, coal and natural gas are proven to create substantial damage to the environment by emitting environmentally harmful gasses that can be hazardous to living organisms in its surrounding and can also result to a global rise in temperature [1]. Due to foreseen damage of using conventional fossil fuels and the need to find alternative sources of energy, renewable energy systems became an integral part of the solution to meet the current and future energy demands without relying on conventional sources. Out of all the renewable energy sources, the energy radiated by the sun is one of the most promising source of clean energy. If harnessed efficiently, the energy radiated by the sun incident to the Earth's surface can provide an enormous amount of energy which is sufficient to meet the world's current and future energy demands [2].

To efficiently harness the sun's light energy, understanding the fundamental properties of light and how to convert it into other more practical forms such as electricity and heat are crucial for engineers and researchers. High efficiency crystalline silicon solar cells are the most widely used solar cell in the industry due to its high conversion efficiency and long-term stability in various weather conditions. In order to produce a high-efficiency solar cell, a good combination of antireflection coating is essential in order to reduce optical reflections and increase the transmission of light in wide range of wavelengths. Selecting the proper combinations materials for antireflection coatings are complex, especially when dealing with multiple layers. Understanding the mathematical equations pertaining antireflection coatings and using it in a simulation software can greatly help researchers in selecting the right combination of materials that will achieve the lowest possible reflectance which results to higher device efficiency.

1.1. Thesis Objectives

The aim of this research is to present the fundamental working principles of crystalline silicon solar cells and antireflection coatings. The basic structure of both solar cell and antireflection coating are thoroughly studied and presented. Various mathematical equations are used in order to measure and simulate the reflectance spectra of different combinations

of commonly used dielectric materials that are used as antireflection coatings for crystalline silicon solar cells.

This study aims to understand the fundamental working principles and mathematical equations of thin films that are used as antireflection coatings on crystalline silicon solar cells. Mathematical equations for single, dual and multi-layered ARC are presented and simulated with the use of MATLAB. Various experimental measurements from different literature are used with the permission of their authors to validate the accuracy of the mathematical equations that are used in this study. In addition, PC1D simulations are also used for validating the reflectance spectra and measuring the performance of solar cells with different combinations of ARC.

1.2. Purpose of the Study

Antireflection coating (ARC) has been an integral part of the modern high efficiency solar cells. It helps to reduce optical losses due to reflection and maximize the transmission of light which results to higher generation rate and higher overall efficiency. Numerous combinations of different dielectric materials have been investigated by various researchers in order to obtain the lowest possible reflection on wide range of wavelengths in the visible spectrum which is the most important spectrum for solar cell operations. Although many papers have been published on the results of different combinations of dielectric materials on different types of solar cells, a paper which thoroughly investigates and presents the step by step mathematical equations that are required in order to measure and simulate the reflectance spectra of different layers of antireflection coatings for solar cells are rare.

I have chosen to work on simulation of antireflection coatings for silicon solar cells because there is limited reference for a thorough explanation on the detailed mathematical equations that are governing the working principles. Understanding the mathematical equations that governs the properties and behavior of light on multilayered thin films on a silicon substrate can greatly help in achieving more efficient solar cells in the future without spending huge amount of money on complicated laboratory experiments that intends to find the best combination of dielectric materials in order to achieve the highest possible efficiency of solar cells. Instead of focusing on experiments on the combination of ARCs, researchers can now focus more on the material, optical and electrical properties of each material that

are used on solar cells and achieve better quality solar cells that can withstand harsh weather conditions and still function efficiently.

1.3. Thesis Outline

This thesis is organized as follows, Chapter 1 presents the general introduction about current issues in renewable energy and photovoltaics industry. Chapter 2 presents the working principles of crystalline silicon solar cells and the performance measurements of solar cell operations. Chapter 3 explains the fundamental working principle behind thin films and antireflection coatings which presents the properties of light and its interactions with other materials. In Chapter 4, various mathematical equations that are governing the reflection and transmission of light in various layers of antireflection coatings on crystalline silicon solar cells are presented. In addition, PC1D simulations are also added in order to present the effect of antireflection coating on the overall efficiency of the solar cell. Chapter 5 presents the conclusions and suggestions for future studies that are related in this work.

1.4. World Energy Consumption

Electricity became an essential part of our modern societies in order to achieve a better quality of life. The demand for electricity is steadily rising due to numerous infrastructures and beneficial activities around the world. According to the World Energy Outlook 2017 published by the International Energy Agency (IEA), the worldwide spending on energy in 2017 alone is more than 2 trillion dollars. This massive amount of money was spent on different types of energy sources such as coal, gas, hydro, solar and other energy sources. The amount is foreseen to continually rise in the future due to the rising worldwide demand for electricity, especially in developing nations [3]. Figure 1 shows the global energy expenditure by source and scenario. New Policy Scenario (NPS) graph considered when various countries adopt different policies and use oil-based products as the main source of energy and electricity while Sustainable Development Scenario (SDS) graph means that majority of countries worldwide will adopt policies to make various renewable energy sources as their primary source of electricity in the future.

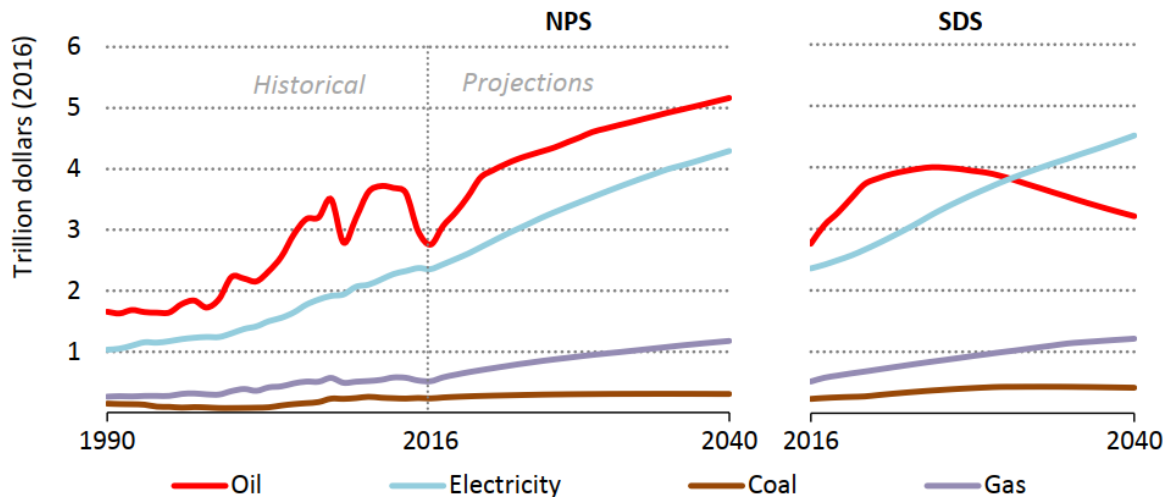


Figure 1. Global energy expenditure by source and scenario [3]

1.5. Importance of Renewable Energy

Our world is facing huge challenge on how to produce sufficient energy without significantly harming our environment. Scientists, researchers and thinkers came to an agreement that the world needs to cut its carbon dioxide emissions in order to prevent or minimize the impact of global warming [1, 4]. The use of conventional energy sources in powerplants, automobiles and other machineries are the primary cause of huge carbon dioxide deposits in our atmosphere which in turn causes a global rise in temperature that causes an increase in natural disasters around the world. This led to a consensus between various developed nations to promote certain policies which will lead to sustainable developments in the future. One of the most important solution in this global crisis is the transition from using traditional energy sources to renewable energy [1].

1.6. Renewable Energy Usage

According to the Renewable Energy Statistics published by International Renewable Energy Agency (IRENA), the use of renewable energy systems skyrocketed in the past few decades amounting to a total capacity of more than 2 million megawatts (MW) in 2016 [5]. This amounts to more than 200% increase in generation capacity compared to 2007. This increase in energy generation capacity corresponds to the fast evolution of renewable energy systems which are becoming more and more cheaper as years pass by and is foreseen to

become more cheaper than conventional energy sources in the near future [3]. Figure 2 shows the total capacity of renewable energy systems worldwide from 2007 to 2016. Among these renewable energy sources, solar or photovoltaic (PV) energy systems has the highest added capacity and foreseen to be the most widely used renewable energy system in 2040 [5].

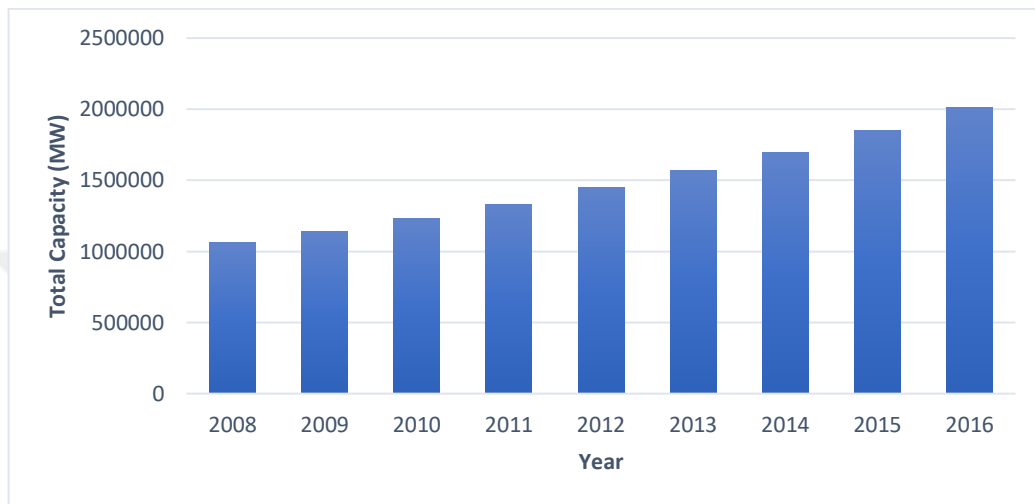


Figure 2. Global renewable energy capacity in MW from 2007 to 2016

Figure 3 shows the global annual average capacity added in the power sector and the forecast of from 2017 to 2040 [3]. Solar PV system is highly sought after by investors due to the rapid decline of the price per MW in the market due to mass production and development of higher efficiency solar cells.

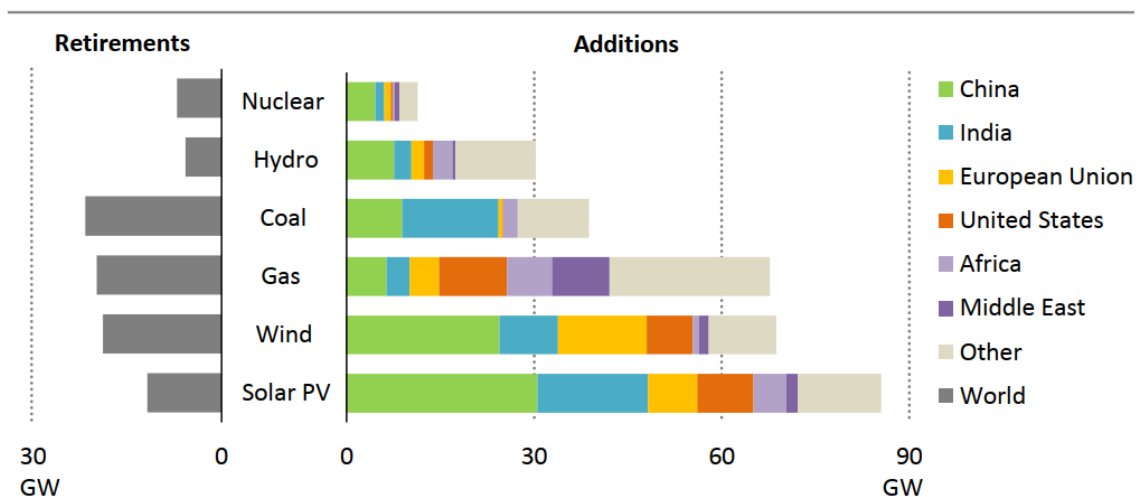


Figure 3. Global average annual capacity additions from 2017 to 2040 [3].

1.7. Solar Cell Efficiencies

Solar cells rapidly evolved since the discovery of photovoltaic effect by the French scientist Edmond Becquerel in 1839 [2]. Enormous amount research are being conducted on combinations of different materials and techniques in order to increase the quality, efficiency, and reduce production costs of each solar cell. These led to the development of various types of solar cells with different structures and combination of materials. Figure 4 shows the timeline of various types of solar cells and their corresponding efficiencies [6].

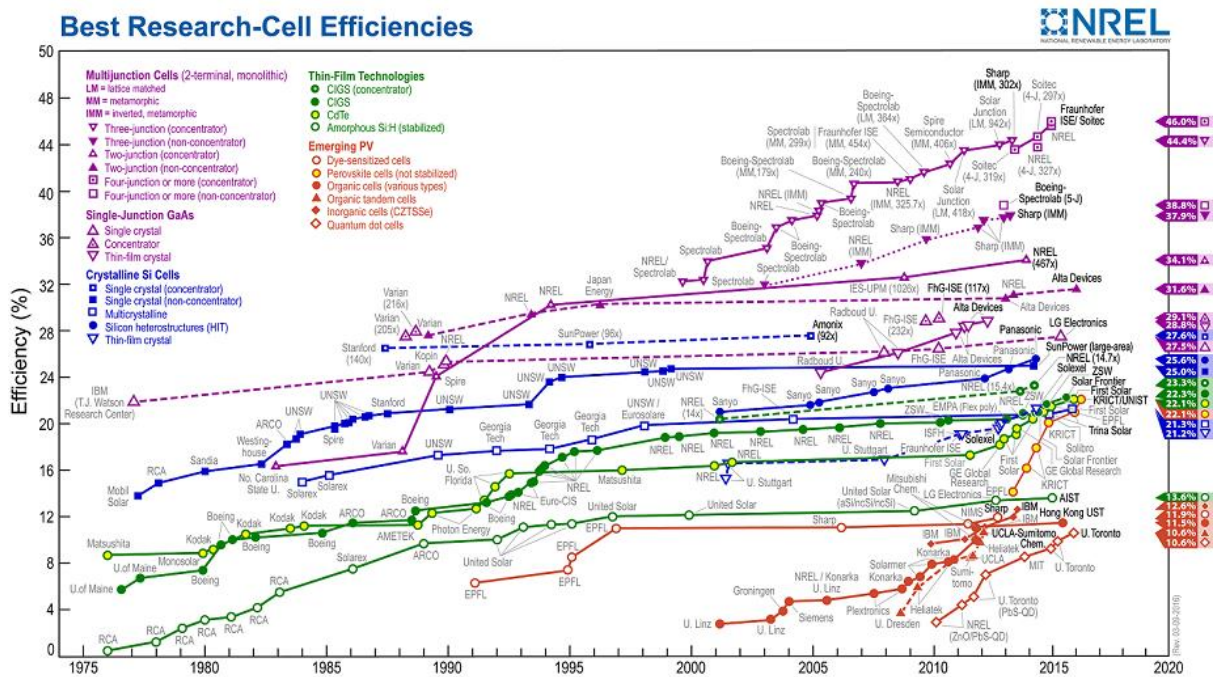


Figure 4. Solar cell efficiency timeline [6]

In this figure, we can see the evolution of efficiencies of various type of solar cells from different universities, research laboratories, and leading manufacturing companies in the solar cell industry worldwide. A solar cell with more than 40% efficiency in standard test conditions is now available and under the developmental stage in leading research laboratory such as Fraunhofer, Soltec, NREL and others.

1.8. Types of Solar Cells

Solar or photovoltaic cell is a semiconductor device which directly converts sunlight into electricity through a phenomenon called photovoltaic effect. Photovoltaic effect is a phenomenon that happens when the energy of a photon that is absorbed by the semiconductor material is larger than the energy of its band gap, thus creating an electron-hole pair which can be collected and converted into electricity. The energy of the photon incident on the surface of the semiconductor material will be absorbed by the semiconductor if its energy is equal or higher than its band gap, the absorbed photon excites an electron to break away from its valence band to conduction band which results in production of excess charge carriers [2, 4].

Solar cells are usually named after the semiconductor materials that are used in its substrate or absorber layer. Some solar cells are designed for terrestrial use while some are optimized for outer space applications. A solar cell can be constructed using a single or multiple layers of different semiconductor materials. Multiple-layered materials have advantage in absorbing wide range of wavelengths of light and have better separating mechanisms of charge carriers. There are many types of solar cells that are available on the market and in developmental stage in various laboratories. These solar cells can be classified into three generations [7, 8].

- *First Generation or conventional solar cells* are made from crystalline silicon. Crystalline silicon solar cells are the most widely used solar cell in the industry today, with a global market share of more than 90%.
- *Second Generation solar cells* are made from different semiconductor materials such as amorphous/thin film silicon, CdTe and CIGS that are made into thin-film solar cells. Thin-film solar cells are widely used in large-scale PV stations and stand-alone PV systems.
- *Third Generation or Emerging Photovoltaics* are solar cells which are still in the development / research phase and are not yet available on the market. Many of these solar cells use organic, organometallic and inorganic materials in order to achieve higher efficiency than the conventional solar cells. Huge investments are made on research and development of these type of solar cells as they have the potential to make a high efficiency, low cost solar cell in the near future.

1.9. Crystalline Silicon (c-Si) Solar Cells

More than 90% of globally produced solar cells are based on crystalline silicon substrate and is by far the most important material in photovoltaics industry [8]. There are two types of crystalline silicon solar cells available in the market, monocrystalline and polycrystalline. Monocrystalline silicon is a crystalline solid material in which the crystal lattice is continuous and unbroken until the boundaries. Polycrystalline silicon or polysilicon is a material that consists of many small monocrystalline grains which are mixed in random orientations. Monocrystalline has one uniform color while polycrystalline has clear random grains that are visible even to the human eye [9]. Monocrystalline silicon solar cell has higher efficiency compared to polycrystalline solar cells due to lesser defects thus having longer recombination time for charge carriers. Figure 5 shows the monocrystalline and polycrystalline solar cell wafers.

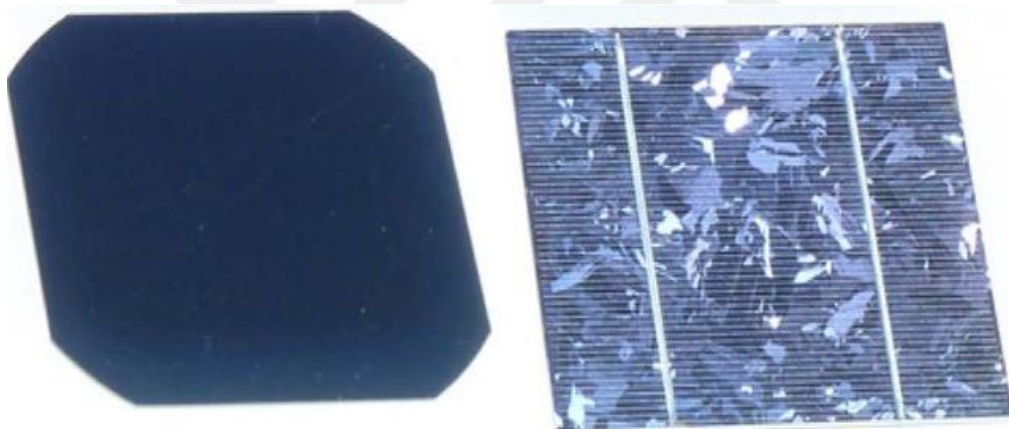


Figure 5. Monocrystalline and polycrystalline silicon wafers [10]

2. WORKING PRINCIPLES OF CRYSTALLINE SILICON SOLAR CELLS

2.1. Structure of c-Si Solar Cells

The basic structure of high efficiency crystalline silicon (c-Si) solar cell is shown in Figure 6. It is composed of front contacts, antireflection coating, emitter layer (N-type), absorber layer (P-type), back surface field and aluminum back contact.

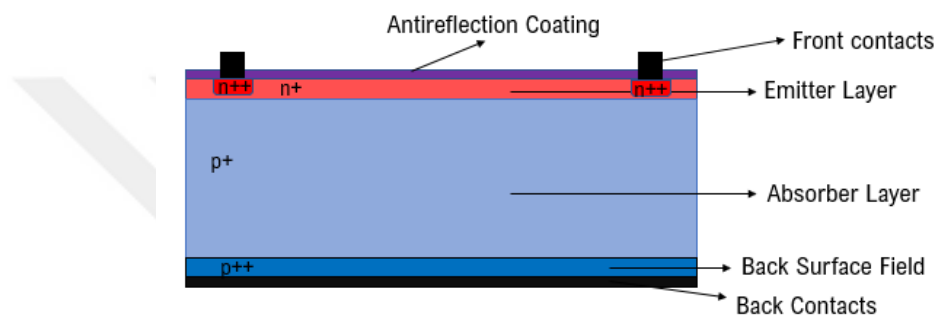


Figure 6. Basic structure of a crystalline silicon solar cell

. Antireflection coating is an additional layer of thin-film that significantly eliminates optical reflections and increase light transmission on the solar cell. Emitter and absorber layers are responsible for generating and transporting charge carriers. Back surface field is a heavily doped layer which acts as a passivation layer at the rear of the solar cell while front and back contacts are the collectors of generated currents that will be carried to the load.

The working principle behind solar cell operation is divided into three important parts. First is the absorption of light that results to generation of electron-hole pair which acts as the mobile charge carriers in the solar cell. Second is the transport mechanism which splits the mobile charge carriers called electrons and holes into the proper section of the solar cell in order to be collected. And the third is collection of electrons and holes which is done by the metal contacts that are situated on the front and back of solar cells and transfer the collected energy into the load. Understanding the fundamental principles of various phenomenon that occurs during these 3 processes and the factors that are affecting them will help us understand and design a more efficient solar cell [2, 9].

2.2. Properties of Light

Sunlight is a form of energy radiated by the sun incident to the Earth's surface which is composed of broad spectrum of electromagnetic waves that includes the visible spectrum that human eye can see as a white bright light. Electromagnetic (EM) waves have frequency of propagation which is inversely proportional to its wavelength. Sunlight also composed of particles that carries a specific amount of energy called photons [2, 9]. Figure 7 shows electromagnetic spectrum with the visible spectrum from infrared to ultraviolet.

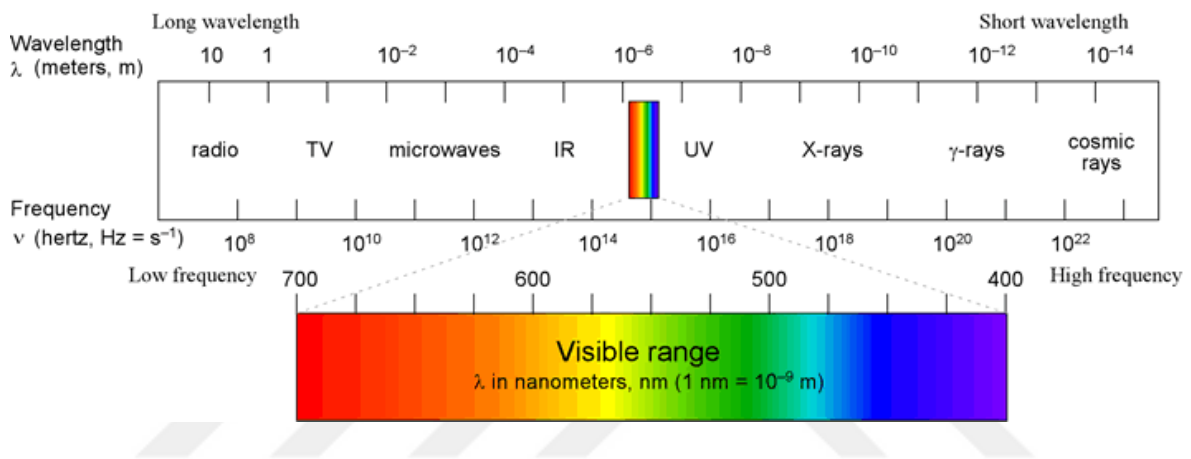


Figure 7. The Electromagnetic spectrum [11]

The most important part of the electromagnetic spectrum for solar cell operation is the visible spectrum. Visible spectrum is situated in the range of 400nm to 700nm which is the effective operating range of typical photovoltaic cells that are available in the market today.

2.3. Photon Flux

Photon flux is the number of photons radiated by a light source per unit area in a given time given by the equation $\Phi = \# \text{ of photons}/\text{cm}^2 \cdot \text{s}$. Photon flux is crucial in determining the carrier generation rate of solar cells. The intensity of photon flux based on AM1.5G spectrum [12, 13] is shown in Figure 8.

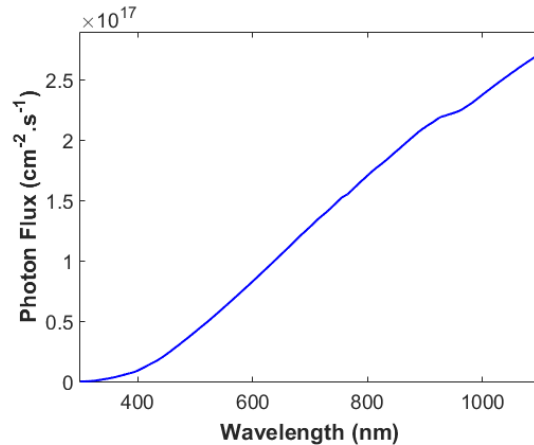


Figure 8. Photon flux based on AM 1.5G spectrum

We can see an almost linear relation between wavelength of light and the number of photons radiated. Higher energy light such as violet and blue lights contains lesser photons compared lower energy lights such as red and infrared which contains huge quantities of photons at a given time.

2.4. Spectral Irradiance

Light waves that reach the Earth's surface has specific power densities that is dependent on wavelength. The energy of photon at a particular wavelength multiplied by the photon flux will yield the power density which is measured in Watts per m²(W/m²) [14], [15]. The power density at a particular wavelength is characterized by the spectral irradiance which is the most commonly used method to characterize a light source. Figure 9 shows the spectral irradiance of the sunlight when it reaches the Earth's surface.

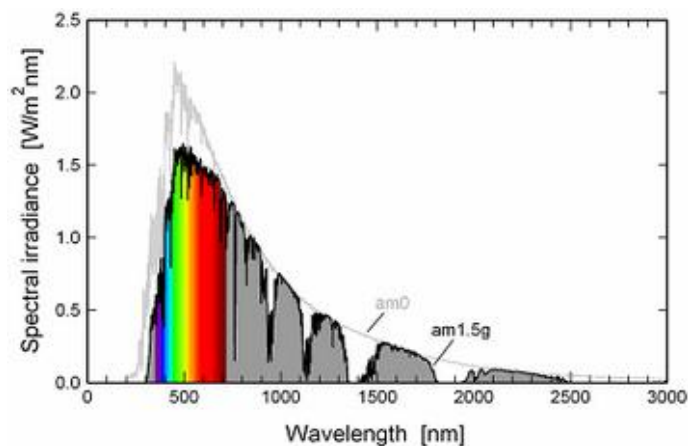


Figure 9. AM 1.5G global spectrum [16]

Knowing the power density in specific wavelength is crucial in selecting materials for designing solar cells in order to effectively convert the energy radiated by the sun. Wavelengths in the range of 500 to 550nm have the highest power density in the visible spectrum. Researchers design antireflection coatings with minimal reflection in these range of wavelengths in order to efficiently convert the high power-density light into electricity.

2.5. Band Gap

Semiconductor materials are unique when it comes to their electrical properties, it can either act as an insulator or conduct electricity depending on external factors that can alter its energy levels. There are three most important energy levels in a semiconductor, the valence band, conduction band, and the band gap. The lowest energy level where the atoms are bonded together and therefore immobile is the valence band. Atoms are strongly bonded to its neighboring atoms, thus become immobile which therefore acts like an insulator. When additional energy is received by a valence electron through external factors such as high energy photons or high temperatures, the electrons on the outer shell can break out of their valence band and become a mobile charge carrier. The band where the electrons can freely move and conduct electricity is called the conduction band. The minimum amount of energy needed for an electron to be released from its covalent bond is called band gap. When a semiconductor is subjected by a light with high enough energy, the electrons in the valence band can break away into conduction band where they can move freely. Electrons that broke away from their covalent bonds leave an empty space called hole which also behaves like an electron but with a positive charge [2, 9]. Figure 10 shows the process of breaking covalent bonds by photon.

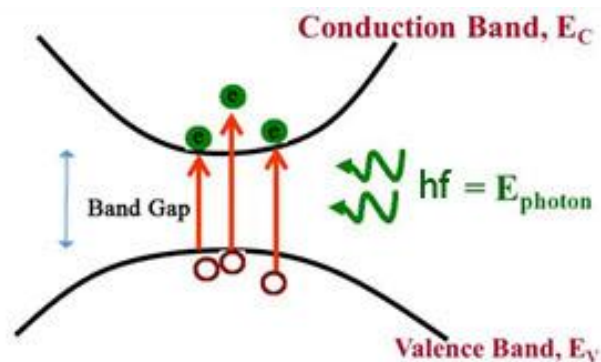


Figure 10. Excitation process from valence to conduction band

Absorbed photon with an energy that is equal or higher than the band gap of semiconductor can generate an electron-hole pair which will become mobile charge carriers. These mobile charge carriers are either transported using various transport mechanisms and collected by the metallic contacts in order to generate electricity or recombine and get back to their stable state.

2.6. Transport Mechanisms

Electrons and holes that are not bonded are considered free moving carriers which needs to be separated in order to prevent recombination and generate electric current. Transport mechanisms are needed in order to move electrons into the negative electrode and holes into the positive electrode. The two main transport mechanisms used in the solar cell operations are called diffusion and drift [17].

2.6.1. Diffusion

Diffusion is the movement of particles due to difference in concentration of carriers in the semiconductor material. When high energy photons are absorbed by the semiconductor material, electron-hole pairs are generated which in turn creates uneven carrier density within the semiconductor. Carriers within the high concentration area tends to move towards the area with lower carrier concentration through diffusion, carriers will continue to do diffuse until the density is uniformly distributed across the material [17, 18]. Figure 11 shows the diffusion process in a semiconductor material.

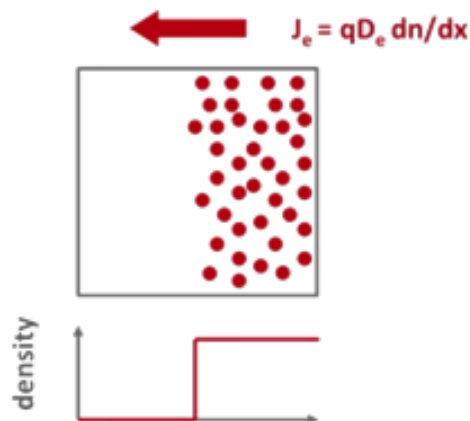


Figure 11. Diffusion of carriers [19]

Doping and generation contributes to uneven charge carrier density throughout the device. Charge carriers move into lower concentration areas until it reaches an equilibrium state where all charge carriers are evenly distributed throughout the device and results to zero net current.

2.6.2. Drift

Another important transport mechanism in a solar cell is the drift. Charge particles such as electrons and holes can also be moved by the influence of an electric field. Drift is a transport mechanism that uses induced electric field in the junctions of two different semiconductor material in order to influence the movement of charge carriers. Holes move towards the direction of the induced electric field while the electrons move in opposite direction of the electric field [18]. Figure 12 shows the movement of charge carriers with an induced electric field.

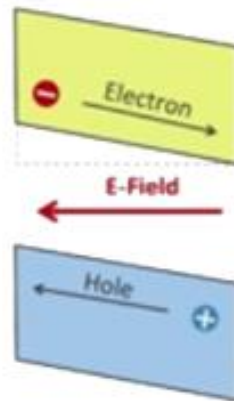


Figure 12. Drift mechanism [20]

When an electron-hole pair is generated by photon, these mobile charge carriers needed to be separated in order to prevent recombination and transported to the collecting electrodes. The induced electric field in the junction of solar cell forces the holes to move into the side where the electric field is induced while the electrons will be pushed in the opposite direction. These electric field also acts as a barrier for the unwanted mobile charge carriers in order prevent recombination.

2.7. Recombination

Electrons which exist in the conduction band are either collected to generate electric current or recombine with holes and lose their energy. Semiconductor materials have three recombination mechanisms. Auger, Shockley-Read-Hall and Radiative recombination [9].

In *Auger recombination*, an electron-hole pair recombines and release its energy to a neighboring free electron in the conduction band, thus exciting it into higher energy level and lose its energy as heat.

Shockley-Read-Hall (SRH) recombination happens due to the various defects that are present in the device. An electron can be trapped in such defects and can recombine with a moving hole thus lose their mobile state [21].

In *Radiative recombination*, electrons and hole recombine directly and emit a photon. Radiative recombination mechanism is usually found in direct band gap semiconductors such as GaAs and InAs and usually negligible on indirect band gap semiconductor such as Silicon and Germanium [22].

The minority carrier lifetime is highly dependent on the recombination rate of the semiconductor material. Minority carrier lifetime sometimes referred to as lifetime is the average time of the carrier in the excited state before it undergoes recombination. Lifetime has a huge effect on the overall efficiency of the solar cell and thus, a key factor in selecting semiconductor materials that used for solar cells.

2.8. PN Junction

The basic working principle most solar cells are based on P-N junction. Impurities are intentionally added to a semiconductor in order to significantly alter its electrical properties. The process of intentionally adding impurities into an intrinsic (pure) semiconductor to alter its electrical property is called doping [9, 18]. The number of charge carriers are directly proportional to the level of doping in a semiconductor material. The majority charge carriers in N-type materials are electrons while in P-type materials, the majority charge carriers are positively charged holes. When joined together, they create a PN junction which is an important part of modern crystalline silicon solar cells [18]. Figure 13 shows the working principle behind PN junction solar cells.

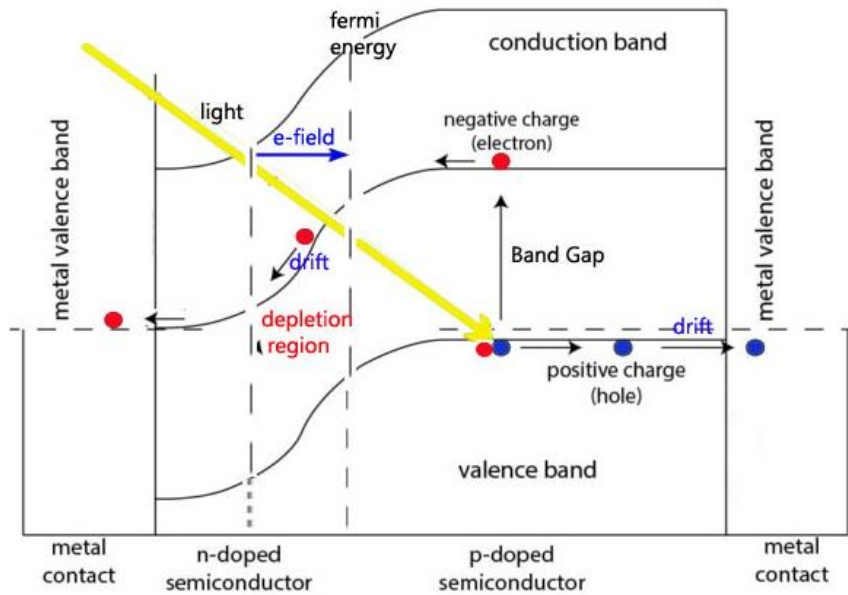


Figure 13. Working principle of PN junction solar cells

The electrons and holes at the junction recombine and forms a region without mobile charge carriers. The area formed between the junction of P and N type where no mobile charge carriers is called the depletion region. The depletion region results to an induced electric field that is in the direction of N region to P region. This induced electric field can influence the movements of minority charge carriers in both region P and N region due to the drift transport mechanism. The minority charge carriers of N region (holes) are transported into the direction of the electric field (N to P) while the electrons in the P region are transported into the direction which is opposite of the electric field. This results to higher number of minority charge carriers in both region which then results to a higher probability of collection by the electrode or metal contact.

2.8.1. PN Junction Without Illumination

Without any illumination, solar cell behaves like a diode. At equilibrium, diffusion and drift currents of both charge carriers are approximately equal thus resulting in a negligible or zero net current. Figure 14 shows the PN junction without illumination.

Although the electric field generated in the depletion region hinders the diffusion of carriers to the other region, some mobile charge carriers with high enough energy can cross

the potential barrier in the depletion region and move into the opposite region thus creating a miniscule amount of current due to diffusion [17, 18].

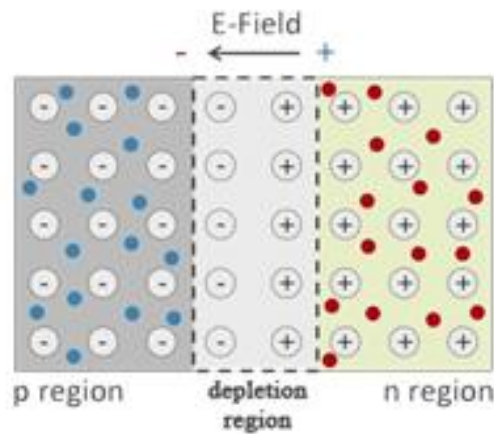


Figure 14. P-N junction without illumination [23]

When a reverse bias voltage is applied, the depletion region gets wider resulting in the increase of electric field and wider potential barrier thus restricting the diffusion of charge carriers. Under forward bias, the depletion region become narrower, thereby decreasing the electric field and barrier potential. In forward bias, an external circuit continuously provides majority charge carriers in both regions thus creating a huge density of charge carrier which results to a net flow of current due to diffusion.

2.8.2. PN Junction Under Illumination

Under illumination, the continuous absorption of photons in a solar cell acts like a current source which generates excess electron-hole pairs and result to an increase of both minority and majority carriers. The number of minority charge carriers significantly increases in both regions during the generation process while the majority charge carriers almost stays the same due to its already huge density. These minority charge carriers are then transported by the help of electric field or the drift transport mechanism. These mobile charge carriers in each region are then collected by electrode (contacts) in front and the back of the solar cell and generate electrical current [2, 18]. Figure 15 shows the working principle of P-N junction under illumination in a solar cell.

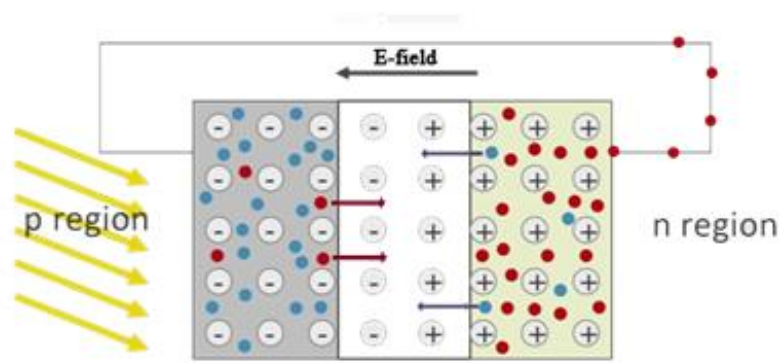


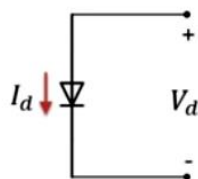
Figure 15. P-N junction under illumination [23]

Generation of electricity in a solar cell involves 3 fundamental processes. First is the generation of electron-hole pairs in the solar cell through the absorption of photons. Second is the separation of charge carriers and transporting them into their desired regions. And third is the collection of charge carriers and transporting it to an external load. Understanding these fundamental processes are needed in order to develop a more efficient solar cell.

2.9. Solar Cell Performance

There are numerous parameters that measures the performance of light to electricity conversion of the solar cell. The four most important metrics of solar cell performance are the short circuit current (J_{sc}), open circuit voltage (V_{oc}), fill factor and efficiency. J_{sc} and V_{oc} are needed in order to plot the IV curve of the solar cell in order to determine the maximum power point (MPP). Figure 16 shows the equivalent circuit of solar cell in the dark and under illumination. [10, 18].

Equivalent circuit of PV cell in the dark



Equivalent circuit of PV cell under illumination

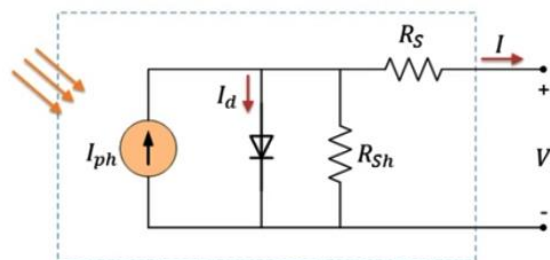


Figure 16. Equivalent circuit of solar cells

I_d corresponds to the diode current, I_{ph} is the current generated by illuminating the solar cell which is based on solar irradiance, R_{sh} is the parasitic shunt resistance due to some defects in the solar cell while R_s is the series resistance which is an inherent property of the metallic contacts and semiconductor materials that are used in the solar cell

2.9.1. Short Circuit Current

Short circuit current (J_{sc}) is the maximum current that can be produced by the solar cell when there's no voltage (short circuited). It is the difference between the total current generated by absorption of photon and the current that is generated by the diode in the dark. Solar cell behaves like a diode when there's no illumination. Under illumination, the light source acts a current source due to its current generating capabilities. J_{sc} can be solved by using the following equations [2, 18].

Ideal diode equations:

$$I_{dark} = I_o \left(e^{\left(\frac{qV}{kT}\right)} - 1 \right) \quad (1)$$

$$I_{sc} = I_{ph} - I_o \left(e^{\left(\frac{qV}{kT}\right)} - 1 \right) \quad (2)$$

$$J_{sc} = \frac{I_{sc}}{A} \quad (3)$$

The total current generated in a solar cell is directly proportional to the area of the solar cell, the larger the area, the higher amount of current will be generated. Another important factor in determining the value of the J_{sc} is the temperature T in kelvins. I_o is the reverse saturation current at temperature T , the value of I_o increases as the temperature rises. The constants V , q and k are voltage across the diode, the electric charge and Boltzmann's constant.

2.9.2. Open Circuit Voltage

The open circuit voltage of a solar cell (V_{oc}) is the maximum voltage that can be obtained when the short-circuit current is zero [12]. The equation of the V_{oc} can be derived when we assume that equation (2) is equal to 0 which we can find in equation (4). In this

equation, the leakage current (J_0) is strongly dependent on temperature, higher temperature will correspond to huge amount of J_0 which then results to a lower value of V_{oc} [24].

$$V_{oc} = \frac{k_b T}{q} \ln \left(\frac{J_{ph}}{J_0} + 1 \right) \quad (4)$$

Two other important factors in the determining the value of V_{oc} is the amount of doping in the semiconductor material and the band gap of the absorber material. Higher amount of doping means larger quantity of mobile carriers and higher electrical field which aids in drift of carriers. Band gap of materials can contribute greatly on the generation rate and rise in temperature on higher wavelengths due to conversion of excess energy of photon into heat.

2.9.3. I-V Curve

I-V curve is a graphical representation of the maximum operating capability of a solar cell on a given irradiance at a specific time. It shows the maximum obtainable current (J_{sc}) and the maximum obtainable voltage (V_{oc}) during the operation of a solar cell. Figure 17 shows the IV curve of a solar cell. We can also see the fill factor which is the largest possible rectangle that can be fitted under the IV curve.

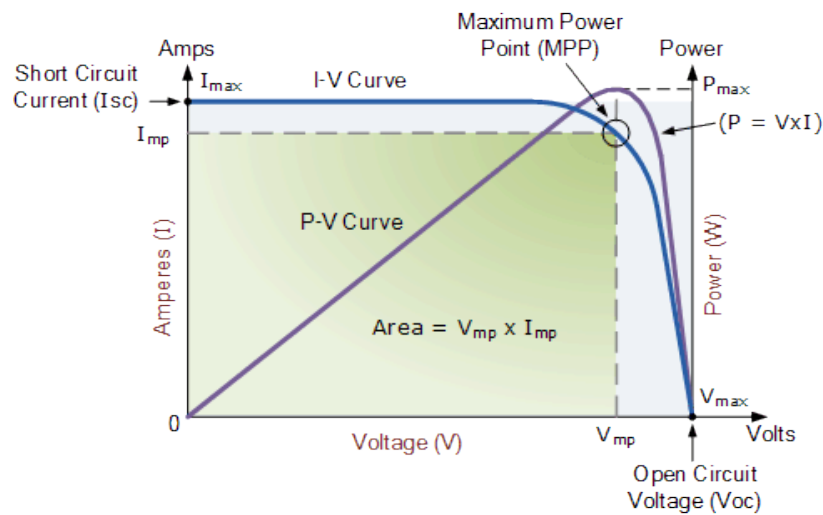


Figure 17. Solar cell IV curve [25]

We can find the maximum power point (MPP) under the IV curve. The maximum power point is the optimal point where the values of I_{sc} and V_{oc} delivers the maximum power. This MPP is important to the operations of a solar cell, to the extent that external devices or circuits are added to the solar cell in order to track the optimum angle of incidence and obtain this point.

2.9.4. Fill Factor

Fill factor (FF) is the ratio between the maximum theoretically obtainable power over the actual maximum obtainable power in a solar cell. Fill factor is the largest possible area that a rectangle can fit under the I-V curve [9, 26]. Equation (5) shows the equation in determining the fill factor of a solar cell.

$$FF = \frac{I_{mp}V_{mp}}{V_{oc}I_{sc}} \quad (5)$$

FF value which is closer to 1 means that the solar cell is operating at optimum conditions.

2.9.5. Efficiency

Efficiency is the most widely used measurement criteria in comparing the performance of different types of solar cells. Efficiency is the ratio of the actual power generated by the solar cell over the actual input energy (irradiance) from the sun. This performance measurement is usually obtained using standard test conditions under 1.5G global spectral irradiance. Equation (6) shows how to determine the efficiency of a solar cell.

$$\eta = \frac{V_{oc}I_{sc}FF}{P_{in}} \quad (6)$$

3. WORKING PRINCIPLES OF ANTI-REFLECTION COATING

Antireflection coating (ARC) is an integral part in designing different types of solar cells. ARC can minimize the reflections of incoming light in specific range of wavelengths which results to a higher generation rate and higher overall efficiency. In order to understand the working principle behind antireflection coatings, we must first understand the nature of light and its interaction with other materials and the equations governing reflection and transmission of light in semiconductor materials.

It is of utmost importance for solar cell designers and researchers to understand both the particle and wave nature of light in order to design a high efficiency solar cell. The Sun's energy which strikes into the Earth's surface and harnessed by solar cells are composed of broad spectrum of electro-magnetic (EM) waves that are combined together and form visible light that have different power densities depending on the wavelength of propagation [2]. The most important region of operation for crystalline silicon solar cell is the visible spectrum.

3.1. Wave Nature of Light

Light is a form of electromagnetic wave that is created from vibrations of electric charges that are traveling through a vacuum at a speed of light. An electromagnetic wave has an inherent property called frequency which is the number of recurring oscillations per unit time. It also has amplitude which has a value equal to the distance from the center to the peak of the oscillation. Wavelength is the distance from one peak amplitude to another [27]. Figure 18 shows the basic characteristics of a wave.

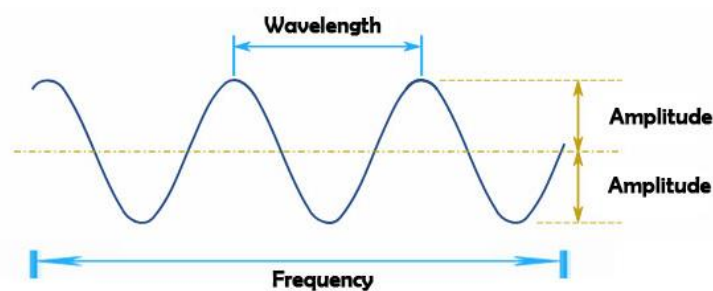


Figure 18. Characteristics of a wave

3.2. Particle Nature of Light

Aside from the wave nature of light, it also consists of energy carrying quantum-mechanical particles called photon. The energy of photon is directly proportional to the frequency of propagation. Energy of photons can be calculated using the equation $E = hc/\lambda = 1.24/\lambda_{(\mu\text{m})}$ where h is the planck's constant and c is the speed of light. High energy photons such as violet and blue lights have high frequency and low wavelengths while low energy photons such as red and infrared have lower frequency and longer wavelengths [28]. Figure 19 shows the type of photons and their wavelength.

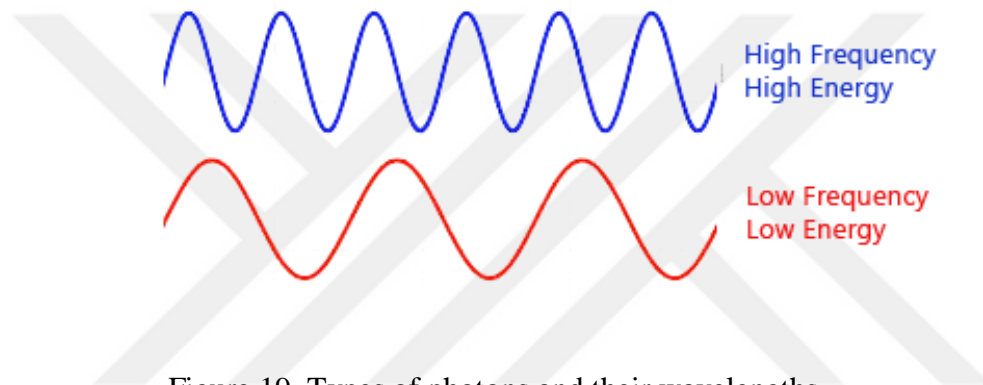


Figure 19. Types of photons and their wavelengths

The frequency of the light is directly proportional to its energy. High energy photons are usually found in high frequency light such as violet and blue while low energy photons are found in red and infrared light.

3.3. Wave Superposition

When two or more waves travel along the same medium at the same time, they can exhibit a phenomenon called wave superposition. As a result, a resultant wave with different amplitude will be formed which is the sum of the amplitudes of both waves. Figure 20 shows the effect of wave superposition.

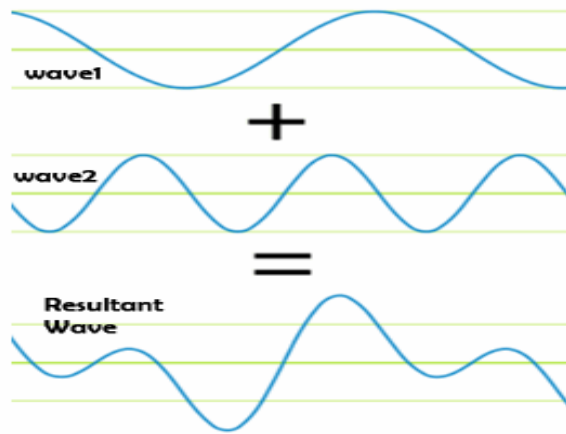


Figure 20. Wave superposition

The amplitude of the resultant wave at a given point in time is equal to the sum of two or more waves with different phase shifts. If two waves will have 180° phase shift with each other, the resultant wave will have zero amplitude.

3.4. Interaction of Waves With Other Materials

Electromagnetic waves travel approximately at a speed of light $c = 3 \times 10^8 \text{ m/s}$ in free space. When an EM wave propagates into another medium with different refractive index, the velocity of propagation (V_p) will be lesser than the speed of light and the wavelength of propagation will also be changed [27]. The frequency of the wave will always be the same regardless of the velocity and wavelength of propagation. The relationship between the velocity of propagation, frequency and wavelength is shown in equation (7).

$$f = \frac{c}{\lambda_0} = \frac{V_p}{\lambda_p} \quad (7)$$

When light travels from free space to a different medium, its velocity of propagation changes and is characterized by its index of refraction (n). Index of refraction is the ratio of the speed of light in free space divided by the speed of light into a denser medium which means that denser materials have lower propagation velocity compared to air.

$$n = \frac{c}{V_p} \quad (8)$$

Where:

f = frequency

c = speed of light (3×10^8 m/s)

λ_0 = wavelength in free space

V_p = velocity of propagation at medium p

λ_p = wavelength of propagation at medium p

n = refractive index

In a medium with higher refractive index, the wavelength of propagation will be wider while the speed of propagation will be slower than the speed of light.

3.5. Absorption of Light

Every semiconductor material has an inherent property to absorb different wavelengths of light which is measured by its absorption coefficient. Absorption coefficient determines the depth which a specific wavelength of light can penetrate the material before it is absorbed. Absorption coefficient is dependent on the dielectric material used and the wavelength of the incoming light [29]. Figure 21 shows the absorption coefficients of commonly used semiconductor materials for photovoltaic applications.

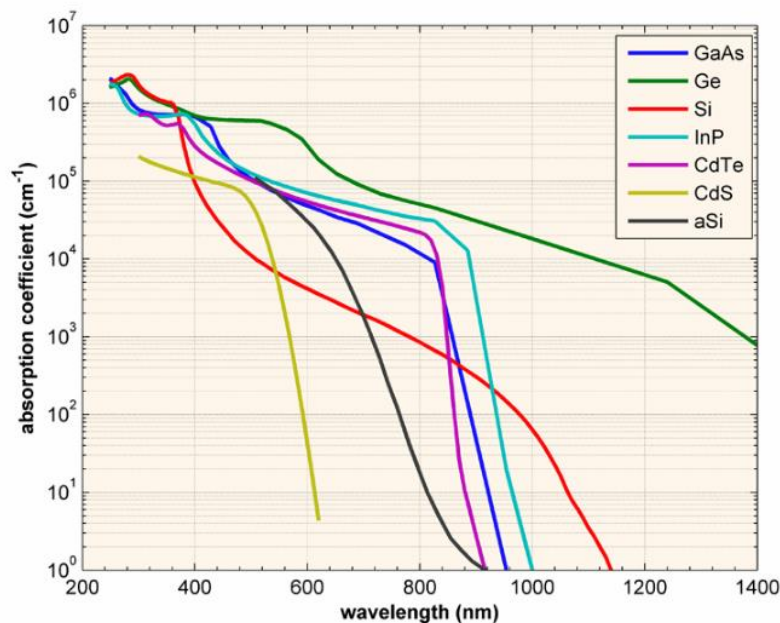


Figure 21. Absorption coefficients of semiconductor materials [29]

Researchers and scientists use the absorption coefficient values of these materials in order to calculate the optimal thickness of solar cells. These values can also be used in

designing the optimal thickness for heterojunction solar cells which combines two or more materials with different band gaps and absorption coefficients.

3.6. Refraction

As the light propagates from one medium to another, the direction of propagation of the light will undergo an effect called refraction (bending) at the boundary of the two materials and change its angle of propagation. The light will be refracted based on the difference of the indices of refraction of the two materials. The quantitative analysis of index of refraction and angle of propagation is characterized by Snell's Law [30]. Figure 22 shows the working principle of the Snell's Law.

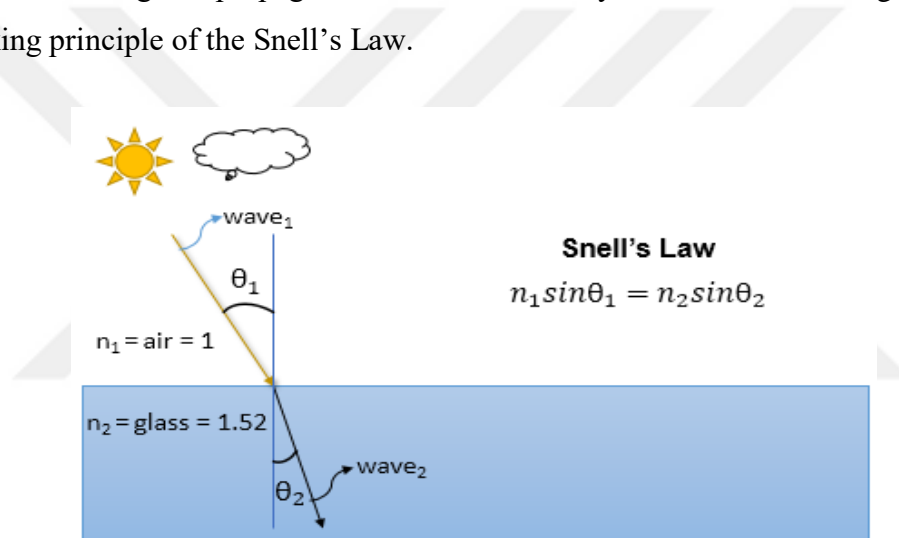


Figure 22. Snell's law

3.7. Refractive Index

Refractive index is the ratio of the velocity of light in free space to that of specific material which is dependent on wavelength. Figure 23 shows the collected data of refractive indices of commonly used materials that are used for antireflection coating [31–37]. Various dielectric materials such as SiN_x , SiO_2 , TiO_2 , ZnS , Al_2O_3 , HfO_2 and others can be used as antireflection coating material in solar cells. Silicon and its composites have been dominating the antireflection coating industry due to its reasonable cost and availability.

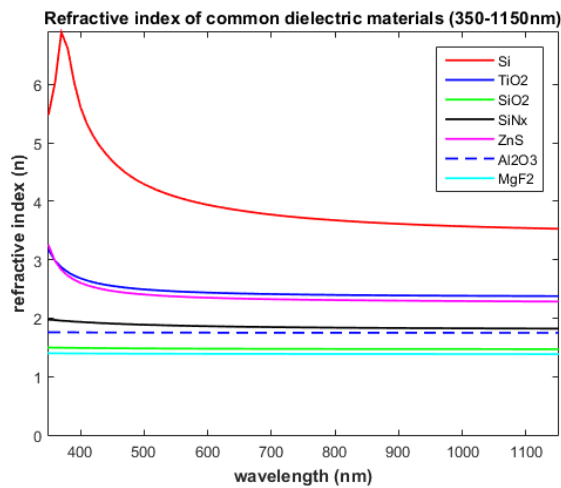


Figure 23. Refractive index of common dielectric materials

The most widely used ARC is Silicon Nitride (SiN_x) and its composites using Plasma-Enhanced Chemical Vapor Deposition (PECVD) due to its excellent surface, bulk passivation and good anti reflection properties [38–41]. They can also be combined into double or multiple layers in order to further reduce the reflections at the surface of the solar cell.

3.8. Reflection

An incident wave that propagates from one medium to another can experience partial reflection and partial transmission depending on the angle of incidence and refractive indices of both materials. Law of reflection states that the angle of incidence will always be equal to the angle of reflection [42]. Additionally, the reflected wave can either be in phase or out of phase depending on the refractive indices of both materials. Figure 24. shows the reflection of waves at a junction of two different mediums.

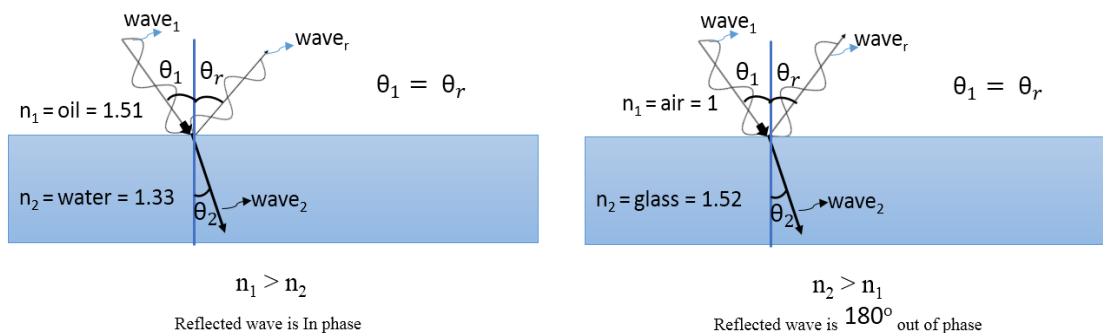


Figure 24. Reflection of waves between two different mediums

If the refractive index of the incident wave (n_1) is less than the refractive index of the 2nd medium (n_2) the reflected wave will be out of phase, or the amplitudes of the two waves will be the inverse of each other. On the other hand, if the refractive index of the 1st medium will be less than the 2nd medium, the reflected wave will be in phase which means that their amplitudes will be the same after reflection [42].

3.9. Polarization

Light is a form of electromagnetic wave which has both electric and magnetic field propagating perpendicularly with each other. The light emitted by the sun incident to the Earth's surface is combination of randomly polarized light or unpolarized light. Polarization determines the direction of the oscillation of an electromagnetic wave. S-Polarization or sometimes known as perpendicular polarization happens when the direction of propagation of electric field is perpendicular to the incident surface while P-Polarization or parallel polarization happens when the electric field is parallel to the incident surface [43]. Figure 25 illustrates the light reflection intensity as a function of incident light in a silicon substrate.

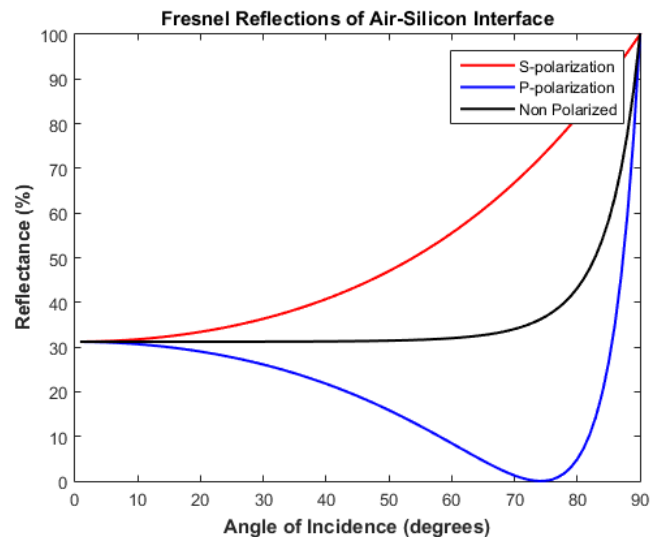


Figure 25. Reflection of polarized and unpolarized light on silicon

The light emitted by the sun is a combination of different wavelengths and polarization combined with each other which results in a white light that can be seen by the human eye. When sunlight hits an interface, i.e. silicon, the intensity of reflection will vary depending on the polarization and angle of incidence.

3.10. Fresnel's Equations

Light is partially reflected and partially transmitted when entering a medium with different refractive index. The intensity of reflection in between two different mediums of propagation can be calculated using Fresnel's equation [44].

The light radiated by the sun is an unpolarized light. In order to calculate the total reflection of an unpolarized light, we must first solve the reflected light using the Fresnel's equation for s and p polarized reflection. Equations (9) to (12) shows Fresnel's equations for coefficient of reflection and transmission of s and p polarized light. Figure 26 shows the Fresnel reflection at interface between two different mediums.

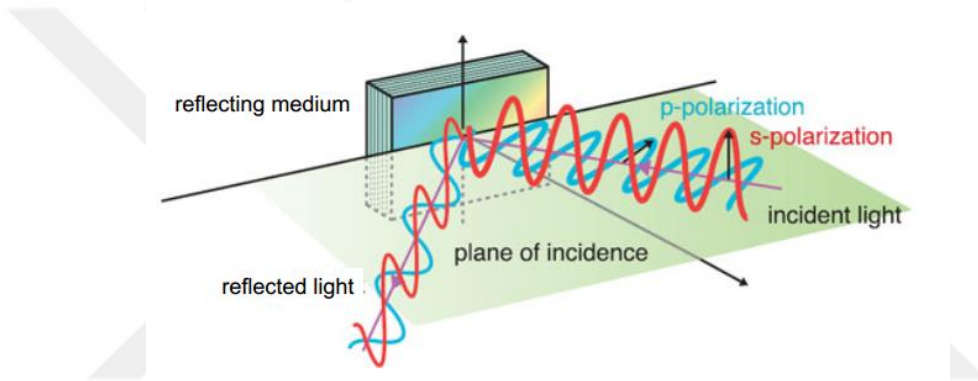


Figure 26. Fresnel reflections [45]

Fresnel's Equations

$$r_s = \frac{n_i \cos \theta_i - n_t \cos \theta_t}{n_i \cos \theta_i + n_t \cos \theta_t} \quad (9)$$

$$r_p = \frac{n_t \cos \theta_t - n_i \cos \theta_i}{n_t \cos \theta_i + n_i \cos \theta_t} \quad (10)$$

$$t_s = \frac{2n_i \cos \theta_i}{n_i \cos \theta_i + n_t \cos \theta_t} \quad (11)$$

$$t_p = \frac{2n_i \cos \theta_i}{n_t \cos \theta_i + n_i \cos \theta_t} \quad (12)$$

Where:

r_s = s-polarized reflectance coefficient

r_p = p-polarized reflectance coefficient

t_s = s-polarized transmission coefficient

t_p = p-polarized reflectance coefficient

n_i = refractive index of incident medium

n_t = refractive index of 2nd medium

θ_i = angle of incidence

θ_t = angle of transmission

4. SIMULATION OF ANTI-REFLECTION COATING

Generation of charge carriers through absorption of photons is the current generating mechanism of solar cells. Efficient absorption of light into the device is of utmost importance in the design of an efficient solar cell. Materials in the solar cell reflect a portion of incident light due to inherent reflectance of the materials used in fabricating solar cells. These reflections can significantly reduce the generation of charge carriers which results to lower efficiency [2, 46]. Figure 27 shows the reflections in different sections of solar cells.

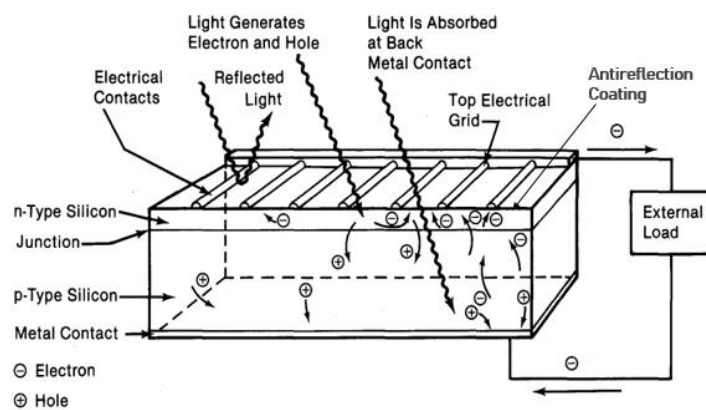


Figure 27. Reflections in solar cells [2]

Antireflection coating is integrated in modern solar cells in order to eliminate or significantly reduce reflections of light in certain wavelengths. Antireflection coating uses combination of thin film dielectric materials with specially calculated thickness that is deposited on top of the substrate in order to eliminate reflections in solar cells. The working principle of antireflection coating is based on thin film interference. Various reflected waves are cancelled through a phenomenon called destructive interference. Reflected waves with 180° phase shift will cancel the other reflected waves, thus resulting in lesser intensity of total reflectance [47]. Figure 28 shows the working principle of constructive and destructive interference.

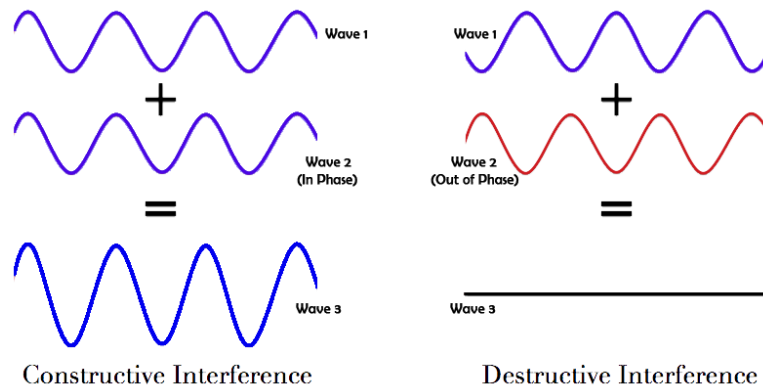


Figure 28. Constructive and destructive interference

If the first and the second wave are in phase, the resultant wave will have higher amplitude due to constructive interference. If both waves have 180° out of phase, then both waves will cancel out each other and have 0 zero amplitude.

4.1. Single Layer Anti-Reflection Coating

A crystalline silicon solar cell without ARC has a high inherent reflection on its surface, more than one third of incident light on its surface is reflected back which results to a significant loss in the overall efficiency due to lesser generation rate [48]. The simplest and the most widely used antireflection coating in crystalline silicon solar cell is the single layer antireflection coating (SLARC). It is composed of a single layer dielectric material such as Silicon Nitride (SiN_x) which is deposited on the top of the silicon substrate. SLARC provides a near-zero reflectance on a specific wavelength. Its thickness is specially calculated in order to achieve the minimum possible reflection in a specific wavelength. The optimum thickness for SLARC is calculated through the equation $d = \lambda_o/4n_1$ where λ_o is the wavelength in free space and n_1 is the refractive index of the first layer ARC [49]. The general working principle of SLARC is shown in Figure 29.

Black arrow indicates transmitted waves while red arrows indicates reflected waves. The total reflection of SLARC is the sum of all reflected waves at the interface of air and ARC. Some reflected waves will be reflected 180° out of phase due to the difference in refractive indices which will induce destructive interference with the other reflected waves. Out of phase waves cancel each other which results to a lower total reflectance.

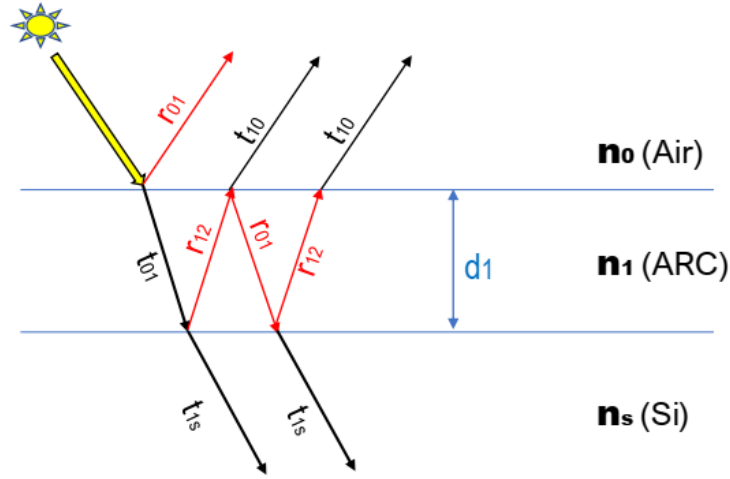


Figure 29. Single layer anti-reflection coating

Fresnel's equation of transmission and reflection of polarized lights are applicable for solving the total reflection at the surface of the ARC. Various equations derived by several authors using different mathematical approaches to solve for the total reflectance are also evaluated. O.S Heaven's equation [50], Transfer Matrix Method [51] and Fresnel's equation using Rouard's method [52] will be used to compute the total reflectance of the SLARC.

Heaven's Equation

$$\delta_1 = \frac{2\pi n_1 d}{\lambda_o} \quad (13)$$

$$\alpha_1 = \frac{2\pi k_1 d}{\lambda_o} \quad (14)$$

$$g_1 = \frac{n_o^2 - n_1^2 - k_1^2}{(n_o + n_1)^2 + k_1^2} \quad (15)$$

$$h_1 = \frac{2n_o k_1}{(n_o + n_1)^2 + k_1^2} \quad (16)$$

$$g_2 = \frac{n_1^2 - n_s^2 + k_1^2 - k_s^2}{(n_1 + n_s)^2 + (k_1 + k_s)^2} \quad (17)$$

$$h_2 = \frac{2(n_1 k_s - n_s k_1)}{(n_1 + n_s)^2 + (k_1 + k_s)^2} \quad (18)$$

$$A = 2(g_1 g_2 + h_1 h_2) \quad B = (g_1 h_2 - g_2 h_1) \quad C = 2(g_1 g_2 - h_1 h_2) \quad D = (g_1 h_2 + g_2 h_1)$$

$$R = \frac{(g_1^2 + h_1^2)e^{2\alpha_1} + (g_2^2 + h_2^2)e^{-2\alpha_1} + A\cos(2\delta_1) + B\sin(2\delta_1)}{e^{2\alpha_1} + (g_1^2 + h_1^2)(g_2^2 + h_2^2)e^{-2\alpha_1} + C\cos(2\delta_1) + D\sin(2\delta_1)} \quad (19)$$

Matrix Method

$$R = \frac{n_1^2(n_0 - n_s)^2(\cos^2 \delta_1) + (n_0 n_1 - n_1^2)^2(\sin^2 \delta_1)}{n_1^2(n_0 + n_s)^2(\cos^2 \delta_1) + (n_0 n_1 + n_1^2)^2(\sin^2 \delta_1)} \quad (20)$$

Fresnel's Equation using Generalized Rouard's Method

Using equations (9)-(13),

For S-Polarization

$$r_{01} = \frac{n_0 - n_1}{n_0 + n_1} \quad (21)$$

$$r_{10} = \frac{n_1 - n_0}{n_1 + n_0} \quad (22)$$

$$r_{12} = \frac{n_1 - n_s}{n_1 + n_s} \quad (23)$$

$$t_{01} = \frac{2n_0}{n_0 + n_1} \quad (24)$$

$$t_{10} = \frac{2n_1}{n_1 + n_0} \quad (25)$$

For P-Polarization

$$r_{01} = \frac{n_1 - n_0}{n_1 + n_0} \quad (26)$$

$$r_{10} = \frac{n_0 - n_1}{n_0 + n_1} \quad (27)$$

$$r_{12} = \frac{n_s - n_1}{n_s + n_1} \quad (28)$$

$$t_{01} = \frac{2n_0}{n_0 + n_1} \quad (29)$$

$$t_{10} = \frac{2n_1}{n_1 + n_0} \quad (30)$$

$$r_1 = r_{01} + [(t_{01}e^{-i\delta_1})(r_{12}e^{-i\delta_1})(t_{10})] + [(t_{01}e^{-i\delta_1})(r_{12}e^{-i\delta_1})(r_{10}e^{-i\delta_1})(r_{12}e^{-i\delta_1})(t_{10})] + \dots \quad (31)$$

$$\text{OR: } r_1 = r_{01} + \frac{t_{01}r_{12}e^{-2\delta_1}}{1 - r_{10}r_{12}e^{-2\delta_1}} \quad (32)$$

$$\text{but } t_{01}t_{10} = r_{01}^2 \quad (33)$$

Thus generally:

$$r_{1(s,p)} = \frac{r_{01} + r_{12}e^{-2\delta_1}}{1 + r_{01}r_{12}e^{-2\delta_1}} \quad (34)$$

$$R = \left| \frac{r_{1(s)}^2 + r_{1(p)}^2}{2} \right| \quad (35)$$

Where:

R = total reflection

n_o = refractive index of air

r_l = reflection coefficient of ARC

n_l = refractive index of substrate

r_{01} = reflectance at interface 0 to 1

k_l = extinction coefficient of ARC

r_{10} = reflectance at interface 1 to 0

k_s = extinction coefficient of substrate

r_{12} = reflectance at interface 1 to 2

d = thickness of the ARC in nm

t_{01} = transmittance at interface 0 to 1

λ_o = wavelength in free space

t_{10} = transmittance at interface 1 to 0

4.1.1. Comparison of Experimental and Simulated SLARC

Figures 30a to 30d shows the reflectance spectra of uncoated and coated silicon solar cell with SLARC using different materials and thickness while Table 1 shows the average reflectance of each device using different methodologies. The values of refractive index n and extinction coefficient k of Silicon [31], TiO_2 [32], SiO_2 [33], and Ta_2O_5 [53] are obtained from online refractive index database [54] and [55].

Experimental measurements were obtained from various authors and used with their permission. Uncoated Si and TiO_2 SLARC are deposited in a double polished FZ p-type Si wafer using Atomic Layer Deposition at 200°C [56]. Ta_2O_5 is deposited in a polished Si substrate using Electron Beam with substrate temperature of 150°C [57]. The measured reflectance spectra were obtained using spectrophotometer.

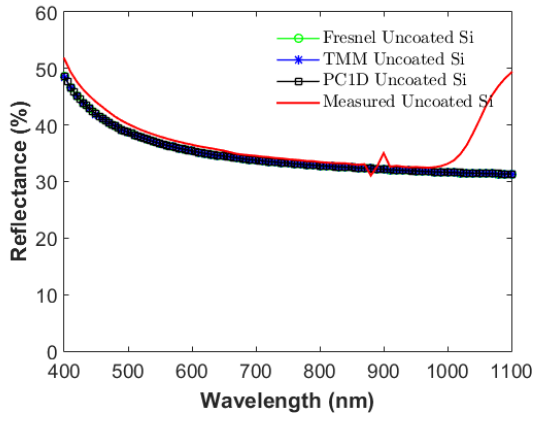


Figure 30a. Uncoated Si solar cell

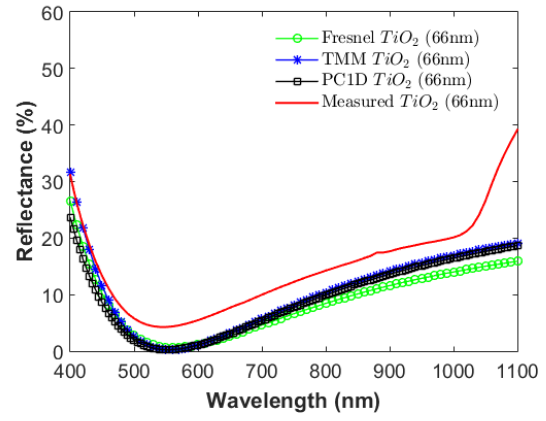
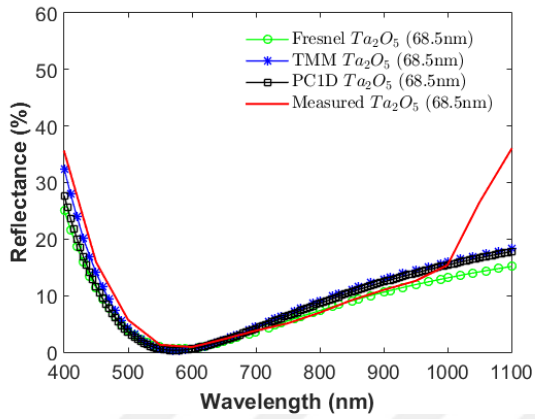
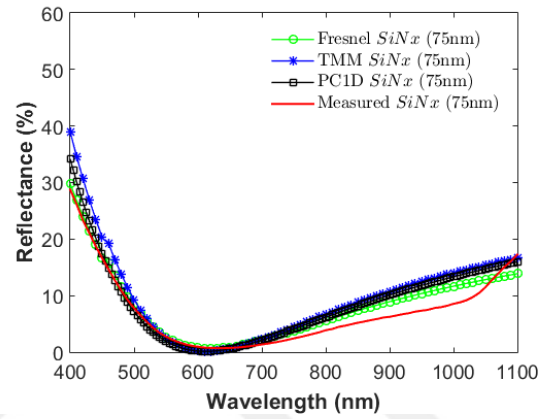
Figure 30b. Solar cell with TiO₂ ARCFigure 30c. Solar cell with Ta₂O₅ ARCFigure 30d. Solar cell with SiN_x ARC

Table 1. Average reflectance of solar cells with and without ARC using different methods

| | Fresnel's Eq. | TMM | PC1D | Measured |
|--------------------------------|---------------|---------|---------|----------|
| Uncoated | 34.7716 | 34.7668 | 34.7396 | 37.1658 |
| TiO ₂ | 8.7598 | 10.4331 | 9.5021 | 14.915 |
| Ta ₂ O ₅ | 7.717 | 9.3931 | 7.9815 | 12.54 |
| SiN _x | 8.0401 | 9.5312 | 8.7532 | 7.1834 |

We can observe in Figures 30a to 30d that both Fresnel's equation using Rouard's method and transfer matrix method can accurately predict the behavior of the reflectance spectra of solar cells with antireflection coatings with different combinations of materials and thickness. A good antireflection coating can reduce the magnitude of reflection down to around 8% which is more than 28% reduction of the total reflection of incoming light.

4.2. Double Layer Anti-Reflection Coating (DLARC)

Single layer ARCs have a disadvantage of only having a minimum reflectance in one wavelength which depends on the design thickness of the ARC. A highly efficient solar cell must have low reflectance in wide range of wavelengths so it can fully utilize the energy emitted by the sun. One of the solution for this problem is having multilayered antireflection coating [57]. Near zero reflections on wide range of wavelengths can be achieved with the use of double layer antireflection coating (DLARC) by utilizing the phenomenon of destructive interference of waves. DLARC have more complex reflections which can interfere with other reflected and transmitted waves and thus result in a lower total reflectance. Figure 31 shows the different interacting waves within the double layer ARC.

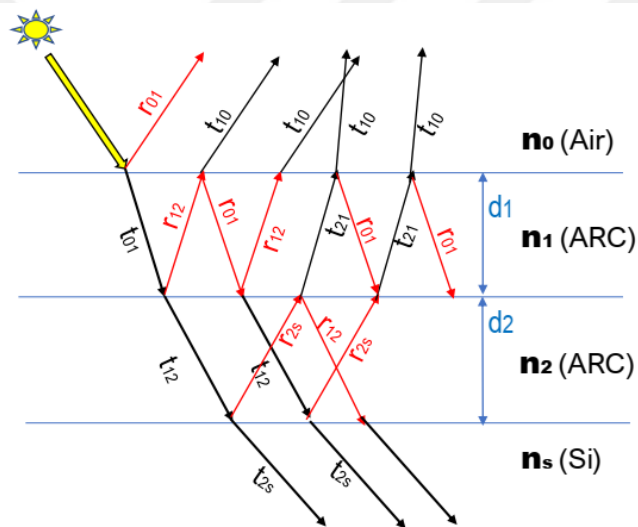


Figure 31. Interacting waves within double layer anti-reflection coating

Double layer antireflection coating has more complex interaction of waves compared to SLARC. Waves in one interface will either be transmitted or reflected which can interfere with other incoming and outgoing waves. The design of the materials and thickness of DLARC is more complicated and the equations are much more complex than SLARC, on the other hand, Fresnel's equations are also applicable to solve for the reflectance and transmittance of the thin film. In this section, Transfer Matrix method and Fresnel's equation using generalized Rouard's method are used to evaluate the total reflectance of DLARC.

Fresnel's Equations using Generalized Rouard's Method

Using Equations in SLARC

$$\delta_1 = \frac{2\pi n_1 d_1}{\lambda_o} \quad (13)$$

$$\delta_2 = \frac{2\pi n_2 d_2}{\lambda_o} \quad (36)$$

$$r_{23s} = \frac{n_2 - n_s}{n_2 + n_s} \quad (37)$$

$$r_{23p} = \frac{n_s - n_2}{n_s + n_2} \quad (38)$$

$$r_2 = r_{01} + [(t_{01}e^{-i\delta_1})(r_{12}e^{-i\delta_1})(t_{10})] + [(t_{01}e^{-i\delta_1})(t_{12}e^{-i\delta_2})(r_{23}e^{-i\delta_2})(t_{21}e^{-i\delta_1})(t_{10})] + \dots \quad (39)$$

or

$$r_{2(s,p)} = \frac{r_{12} + r_{23}e^{-2\delta_2}}{1 + r_{12}r_{23}e^{-2\delta_2}} \quad (40)$$

$$r_{1(s,p)} = \frac{r_{01} + r_2e^{-2\delta_1}}{1 + r_{01}r_2e^{-2\delta_1}} \quad (41)$$

$$R = \left| \frac{r_{1(s)}^2 + r_{1(p)}^2}{2} \right| \quad (35)$$

Where:

R = total reflection

λ_o = wavelength in free space

d_1 = thickness of 1st layer ARC in nm

r_1 = reflection coefficient of ARC

d_2 = thickness of 2nd layer ARC in nm

r_{23} = reflectance at interface 2 to 3

Transfer Matrix Method for DLARC

$$R = \frac{n_0^2 \left[\cos \delta_1 \cos \delta_2 - \frac{n_2}{n_1} \sin \delta_1 \sin \delta_2 \right]^2 + (n_0 n_s)^2 \left[\frac{\cos \delta_1 \sin \delta_2}{n_2} + \frac{\cos \delta_2 \sin \delta_1}{n_1} \right]^2 + [n_1 \sin \delta_1 \cos \delta_2 + n_2 \sin \delta_2 \cos \delta_1]^2 + n_s^2 \left[\cos \delta_1 \cos \delta_2 - \frac{n_1}{n_2} \sin \delta_1 \sin \delta_2 \right]^2 - 2n_0 n_s}{n_0^2 \left[\cos \delta_1 \cos \delta_2 - \frac{n_2}{n_1} \sin \delta_1 \sin \delta_2 \right]^2 + (n_0 n_s)^2 \left[\frac{\cos \delta_1 \sin \delta_2}{n_2} + \frac{\cos \delta_2 \sin \delta_1}{n_1} \right]^2 + [n_1 \sin \delta_1 \cos \delta_2 + n_2 \sin \delta_2 \cos \delta_1]^2 + n_s^2 \left[\cos \delta_1 \cos \delta_2 - \frac{n_1}{n_2} \sin \delta_1 \sin \delta_2 \right]^2 + 2n_0 n_s} \quad (42)$$

4.2.1. Comparison of Measured and Simulated DLARC

Figures 32a and 32b shows the reflectance spectra of solar cell with double layer ARC. Table 2 shows the average reflectance of each device using various methodologies. The values of MgF_2 [35], ZnS [37] and $SiNx$ [34] are also obtained from [54] and [55].

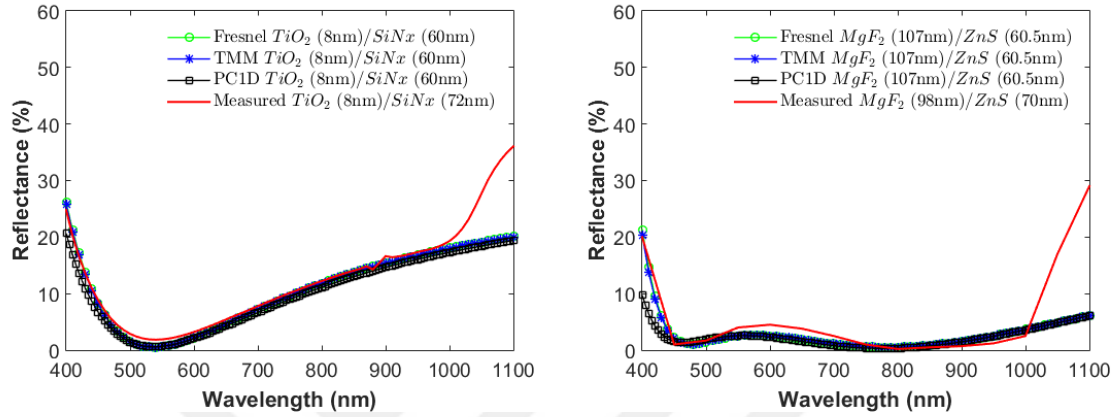


Figure 32a. Solar cell with $TiO_2/SiNx$ ARC Figure 32b. Solar cell with MgF_2/ZnS ARC

Table 2. Average reflectance of solar cells with DLARC using different methods

| | Fresnel's Eq. | TMM | PC1D | Measured |
|---------------|---------------|---------|---------|----------|
| SiO_2/TiO_2 | 11.8753 | 12.9545 | 11.9928 | 7.7746 |
| $TiO_2/SiNx$ | 10.889 | 10.8479 | 10.0345 | 12.7294 |
| MgF_2/ZnS | 2.8016 | 2.7549 | 2.2228 | 5.9733 |

A single layer ARC can only reduce the reflectance to almost zero at a certain wavelength. In order to further reduce the reflections in wider range of wavelengths, double or multi-layer ARC are needed. Careful selection of materials is crucial in order to achieve the minimum possible reflectance in wider range of wavelengths. MgF_2/ZnS combination achieved the best result with less than 3% overall reflectance based on simulation results. A combination of lower refractive index material as the outer layer and higher refractive index at the bottom layer can result to lower average reflectance in wider range of wavelengths compared to SLARC.

4.3. Multi Layer Anti-Reflection Coating (MLARC)

Further reduction of reflectance can be achieved by stacking multiple thin films with different refractive index and thickness on top of each other. Multiple near-zero reflectance at various wavelengths can be achieved by using MLARC. Incoming and outgoing waves interact and cancel each other which results to a better reflectance spectra in wide range of wavelengths in the visible spectrum. But as the number of stacked thin films grow, the mathematical equations that are used for simulating the reflectance spectra of the MLARC is also becoming more complex. Only the Fresnel's Equation using Rouard's model can easily calculate the reflectance spectra of multiple stack of dielectric thin films due to it's simplified mathematical approach. Figure 33 shows the interacting waves in solar cell with MLARC.

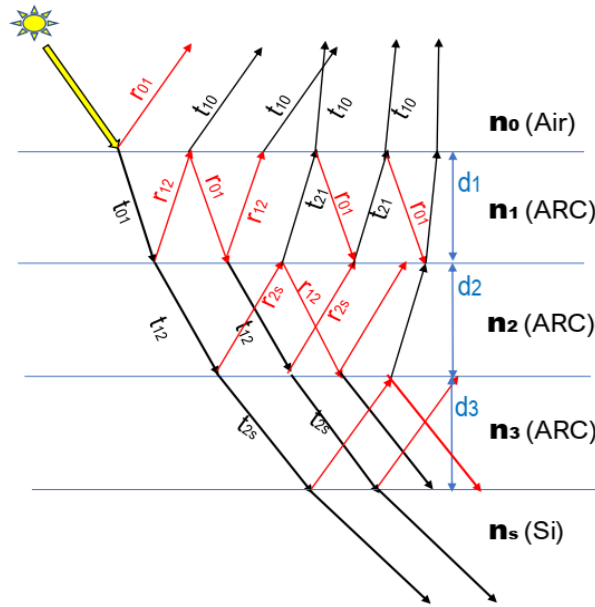


Figure 33. Interacting waves within solar cell with MLARC

Fresnel's Equations using Generalized Rouard's Method

For k number of layers:

$$\delta_k = \frac{2\pi n_k d_k \cos\theta_k}{\lambda_0} \quad (43)$$

Only for the kth layer:

$$r_{k(s,p)} = \frac{(r_{k-1,k}) + (r_{k,k+1})e^{-2i\delta_k}}{1 + (r_{k-1,k})(r_{k,k+1})e^{-2i\delta_k}} \quad (44)$$

For k-1 layer until k = 2:

$$r_{k(s,p)} = \frac{(r_{k-1,k}) + (r_k)e^{-2i\delta_k}}{1 + (r_{k-1,k})(r_k)e^{-2i\delta_k}} \quad (45)$$

$$r_{1(s,p)} = \frac{r_{0,1} + r_2e^{-2i\delta_1}}{1 + r_{0,1}r_2e^{-2i\delta_1}} \quad (46)$$

$$R = \left| \frac{r_{1(s)}^2 + r_{1(p)}^2}{2} \right| \quad (35)$$

4.3.1. Simulation of Alternative MLARCs

Alternative Multi-Layer ARC simulations using combination of 3 layers of antireflection coating on silicon substrate are shown in figures 34a and 34b. Table 3 shows the average reflectance of each device using different methodologies.

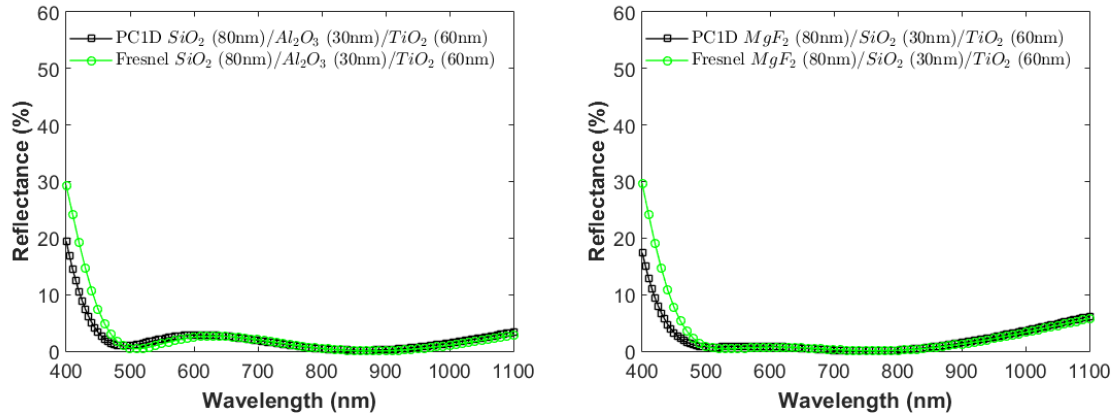


Figure 34a. Solar cell with SiO₂/Al₂O₃/TiO₂ Figure 34b. Solar cell with MgF₂/SiO₂/TiO₂

Table 3. Average reflectance of solar cells with MLARC

| | Fresnel's Eq. | PC1D |
|--------------------------------------------------------------------|---------------|--------|
| SiO ₂ /Al ₂ O ₃ /TiO ₂ | 2.7205 | 2.1886 |
| MgF ₂ /SiO ₂ /TiO ₂ | 2.7987 | 2.0542 |

A good multi-layer antireflection coating can achieve lesser reflectance specially in high spectral irradiance wavelengths. A high refractive index TiO₂ [32] with a refractive index of 2.593 is used as the bottom layer of the ARC. MgF₂/SiO₂/TiO₂ combination

achieved the best results in device performance due to very low reflectance at wavelengths with high spectral irradiance.

4.4. PC1D Simulations

A solar cell simulation software PC1D created by Clungston and Basore [58] of Photovoltaics Special Research Centre at University of New South Wales is used in order to investigate the effects of ARC on efficiency of a c-Si solar cell. PC1D simulation software is used by trusted photovoltaics experts in their papers on various refereed journals [59, 60]. Different combinations of ARC on figures 30a to 34b are simulated on a modern solar cell in order to measure the performance of the solar cell. Same parameters are applied on a single solar cell with different combinations of ARC. The device parameters that are used in simulations are shown in Table 4. The parameters that are used in this simulation is the same with that of typical commercial solar cells which includes series and shunt resistance, texturing, back surface field and others. Table 5 shows the performance of each device with ARC.

Table 4. Solar cell device parameters using PC1D

| | |
|-------------------------------|-----------------------------------------|
| Front surface texture depth | 3 μm |
| Internal optical reflectance | Enabled |
| Series Resistance | 0.8 Ω |
| Shunt Resistance | 50000 Ω |
| Emitter Sheet Resistance | 60 Ω/square |
| Thickness | 180 μm |
| Intrinsic concentration @300k | $1 \times 10^{10} \text{ cm}^{-3}$ |
| P-type background doping | $1 \times 10^{19} \text{ cm}^{-3}$ |
| Front diffusion (N-type) | $2 \times 10^{20} \text{ cm}^{-3}$ peak |
| Rear diffusion (P-type) | $3 \times 10^{18} \text{ cm}^{-3}$ peak |
| Front SRV | $2 \times 10^5 \text{ cm/s}$ |
| Rear SRV | $1 \times 10^6 \text{ cm/s}$ |
| Bulk recombination | $\tau_n = \tau_p = 30 \mu\text{s}$ |
| Temperature | 25°C |
| Device Area | 1 cm^2 |

Table 5. Device performance of Solar Cells with different ARC

| | Materials (nm) | J_{sc} (mA/cm ²) | V_{oc} (mV) | J_{mp} (mA/cm ²) | V_{mp} (mV) | FF | η (%) |
|----------|------------------------------------------------------------------------------------|-----------------------------------|------------------|-----------------------------------|------------------|------|------------|
| Uncoated | Bare Silicon | 24.84 | 603.8 | 24.11 | 514.2 | 0.83 | 12.4 |
| SLARC | TiO ₂ (66) | 36.36 | 612.6 | 34.77 | 503.3 | 0.79 | 17.5 |
| | Ta ₂ O ₅ (68.5) | 36.46 | 612.7 | 34.81 | 502 | 0.78 | 17.55 |
| | SiN _x (75) | 37.5 | 610 | 34.95 | 507 | 0.77 | 17.72 |
| DLARC | TiO ₂ (8)/SiN _x (60) | 36.14 | 612.4 | 33.74 | 514.8 | 0.79 | 17.37 |
| | MgF ₂ (107)/ZnS (60.5) | 38.9 | 614.3 | 36.7 | 510.1 | 0.78 | 18.72 |
| MLARC | SiO ₂ (80)/Al ₂ O ₃ (30)/TiO ₂ (60) | 38.8 | 614.3 | 36.67 | 509.3 | 0.78 | 18.68 |
| | MgF ₂ (79)/SiO ₂ (35)/TiO ₂ (55) | 39.03 | 614.4 | 36.75 | 511 | 0.78 | 18.78 |

An uncoated solar cell reflects more than 34% of light due to inherent reflective properties of silicon. A solar cell with TiO₂ or Ta₂O₅ single layer ARC can reduce the reflection down to 7.1% and increase the efficiency to more than 42% compared to uncoated solar cells. Further decrease in reflectance is achieved by using MgF₂/ZnS as double layer ARC and MgF₂/SiO₂/TiO₂ as multi-layer ARC. Minimum reflectance and maximum efficiency are achieved with multi-layer ARC which has 52.3% more efficiency compared to uncoated solar cell.

5. CONCLUSIONS AND RECOMMENDATIONS

In this study, theoretical and experimental measurements were compared and presented in a graphical format. Experimental measurements with different combinations of materials for antireflection coatings from different researchers validated the theoretical equations used in this study. In addition, one of the most widely used and trusted simulation software PC1D is also used to further validate the accuracy of the theoretical equations that are presented. Figures 29a to 34b shows the comparison of the output reflectance spectra of various solar cells with different combinations of ARC using Fresnel's equation, transfer matrix method, PC1D simulation and experimental measurements. The equations can accurately predict the behavior of reflectance spectra of antireflection coatings with different combinations of dielectric materials with different thickness.

Various data that are available in online database shows the difference in the values of n and k of the same material by using different deposition techniques and parameters such as annealing temperature. Greater accuracies can be achieved by using data with the same material properties, parameters and deposition techniques. A combination of a lower refractive index materials such as MgF_2 or SiO_2 with refractive index of less than 1.5 can be a good first layer while higher refractive index materials such as TiO_2 and ZnS are good materials at the bottom layer. Combination of materials with lower refractive index to higher refractive index in ascending order can have achieve a lower reflectance spectra on wide range of wavelengths.

We recommend future researchers to further study and possibly add the effects of different texturing techniques and light trapping to the reflectance spectra of various solar cells. Refractive index and absorption coefficients of various alternative dielectric materials using different deposition techniques should also be measured and stored in a single database in order to further widen the range of available combinations and achieve greater accuracy.

6. REFERENCES

1. International Renewable Energy Agency, Perspectives for the Energy Transition – Investment Needs for a Low-Carbon Energy System, https://www.irena.org/-/media/Files/IRENA/Agency/Publication/2017/Mar/Perspectives_for_the_Energy_Transition_2017.pdf. 29-Nov-2018.
2. Solar Energy Research Institute, Basic Photovoltaic Principles, U.S. Government Printing Office, Washington D.C., 1982.
3. International Energy Agency, World Energy Outlook 2017, <https://www.iea.org/weo2017/>. 29-Nov-2018.
4. Solanki C.S., Solar Photovoltaics: Fundamentals, Technologies and Applications, Third Edition, Prentice Hall, Delhi, 2009.
5. IRENA, Renewable Energy Statistics 2017. The International Renewable Energy Agency, Abu Dhabi, 2017.
6. National Renewable Energy Laboratory, Research Cell Efficiency Records, Department of Energy. . <https://www.energy.gov/eere/solar/downloads/research-cell-efficiency-records>. 28-Nov-2018.
7. Askari, M.B., Vahid, M. M. A., and Mohsen, M., Types of Solar Cells and Application, American Journal of Optics and Photonics, 3, 5 (2015) 94.
8. Battaglia, C., Cuevas, A., and De Wolf, S., High-Efficiency Crystalline Silicon Solar Cells: Status and Perspectives, Energy and Environmental Science, 9, 5 (2016) 1552–1576.
9. Fonash, S., Solar Cell Device Physics, 2nd Edition, Academic Press, Burlington USA, 2010.
10. Ogbomo, O. O., Amalu, E. H., Ekere, N. N., and Olagbegi, P. O., A Review of Photovoltaic Module Technologies for Increased Performance in Tropical Climate, Renewable and Sustainable Energy Review, 75, 3 (2017) 1225–1238.

11. Electromagnetic Radiation and Waves.
<http://guweb2.gonzaga.edu/faculty/cronk/CHEM101pub/EM-waves.html>. 28 Nov 2018.
12. ASTM G173-03(2012), Standard Tables for Reference Solar Spectral Irradiances: Direct Normal and Hemispherical on 37° Tilted Surface, ASTM International, West Conshohocken, PA, 2012.
13. Spectrum Library. <https://www2.pvlighthouse.com.au/resources/optics/spectrum-library/spectrum-library.aspx>. 13 Dec 2018.
14. Hofstetter, J., Cafiizo, C., and Luque, A., Optimisation Of SiNx:H Anti-Reflection Coatings for Silicon Solar Cells, 2007 Spanish Conference on Electron Devices, February 2007, Madrid, 131–134.
15. Honsberg, C., and Bowden, S., Photon Flux.
<https://www.pveducation.org/pvcdrom/properties-of-sunlight/photon-flux>. 28 Nov 2018.
16. The Global Standard Spectrum (AM1-5G).
[https://www2.pvlighthouse.com.au/resources/courses/altermatt/The Solar Spectrum/The global standard spectrum \(AM1-5g\).aspx](https://www2.pvlighthouse.com.au/resources/courses/altermatt/The%20Solar%20Spectrum/The%20global%20standard%20spectrum%20(AM1-5g).aspx). 28 Nov 2018.
17. Honsberg, C., and Bowden, S., Carrier Transport.
<https://www.pveducation.org/pvcdrom/carrier-transport>. 28 Nov 2018.
18. Isabella, O., Jäger, K., Smets, A., van Swaaij, R.A.C.M.M., and Zeman, M., Solar Energy: The Physics and Engineering of Photovoltaic Conversion, Technologies and Systems. UIT Cambridge, 2016.
19. Honsberg, C., and Bowden, S., Diffusion. <https://www.pveducation.org/pvcdrom/pn-junctions/diffusion>. 28 Nov 2018.
20. Smets, A., Transport of Charge Carriers | 2.3 Charge Carriers | ET3034x Courseware | edX. https://courses.edx.org/courses/course-v1:DelftX+ET3034x+2T2018/courseware/16c43161b8ab43948d0873b11879ce3c/0a551beca1064964807d9a53ea28ebfa/4?activate_block_id=block-v1%3ADelftX%2BET3034x%2B2T2018%2Btype%40vertical%2Bblock%404b157b2b1e3a40e0acc8c40da6da5. 28 Nov 2018.

21. Shockley, W., and Read, W. T., Statistics of the Recombinations of Holes and Electrons, *Physical Review Journals*, 5, 87 (1952) 835–842.
22. Honsberg, C., and Bowden, S., Types of Recombination. <https://www.pveducation.org/pvcdrom/pn-junctions/diffusion>. 28 Nov 2018.
23. Smets, A., Semiconductor Junction II - The Solar Cell | 2.4 Semiconductor Junction | ET3034x Courseware | edX. https://courses.edx.org/courses/course-v1:DelftX+ET3034x+2T2018/courseware/16c43161b8ab43948d0873b11879ce3c/296516f3e6c14e2bb8239e813c574588/3?activate_block_id=block-v1%3ADelftX%2BET3034x%2B2T2018%2Btype%40vertical%2Bblock%40ae5ab926aba34b74bf09dfb54d252. 28 Nov 2018.
24. Levy, M.Y., and Honsberg, C. B., Rapid and Precise Calculations of Energy and Particle Flux for Detailed-Balance Photovoltaic Applications, *Solid. State Electronics*, 7-8, 50 (2006) 1400-1405.
25. Solar Cell I-V Characteristic and Solar I-V Curves. <http://www.alternative-energy-tutorials.com/energy-articles/solar-cell-i-v-characteristic.html>. 28 Nov 2018.
26. Smets, A.H.M., Isabella, O., Jäger, K., van Swaij, R.A.C.M.M., and Zeman, M., *Solar Energy: Fundamentals, Technology, and Systems*, First Edition, UIT Cambridge Ltd., Cambridge England, 2016.
27. Espinoza, F., *Wave Motion as Inquiry: The Physics and Applications of Light and Sound*, Springer International Publishing, 2017.
28. Al-Turk, S., *Analytic Optimization Modeling of Anti-Reflection Coatings for Solar, Matrix*, Master Thesis, McMaster University, Department of Engineering Physics, Hamilton Canada, 2011.
29. Honsberg, C., and Bowden, S., Absorption Coefficient | PVEducation. <https://www.pveducation.org/pvcdrom/absorption-coefficient>. 28 Nov 2018.
30. Tien, P. K., Light Waves in Thin Films and Integrated Optics, *Applied Optics*, 10, 11 (1971) 2395-2413.
31. Green, M. A., Self-Consistent Optical Parameters of Intrinsic Silicon at 300 K Including Temperature Coefficients, *Solar Energy Materials and Sol Cells*, 92, 11 (2008) 1305–1310.

32. Richards, B. S., Single-material TiO₂ double-layer antireflection coatings, *Solar Energy Materials and Solar Cells*, 79, 3 (2003) 369–390.
33. Gao, L., Lemarchand, R., and Lequime, M., Refractive Index Determination of SiO₂ Layer in the UV/Vis/NIR Range: Spectrophotometric Reverse Engineering on Single and Bi-Layer Designs, *Journal of European Optical Society*, 8 (2013).
34. Baker-Finch, S. C., and McIntosh, K. R., Reflection of Normally Incident Light from Silicon Solar Cells with Pyramidal Texture, *Progress in Photovoltaics: Research and Applications*, 19 (2016) 406–416.
35. Dodge, M. J., Refractive Index of Magnesium Fluoride, *Applied Optics*, 23, 12 (1984) 1980–1985.
36. Wood, D. L., Nassau, K., Kometani, T. Y., and Nash, D. L., Optical Properties of Cubic Hafnia Stabilized with Ytria, *Applied Optics*, 29 (1990) 604–607.
37. Siqueiros, J. M., Machorro, R., and Regalado, L. E., Determination of the Optical Constants of MgF₂ and ZnS from Spectrophotometric Measurements and the Classical Oscillator Method, *Applied Optics*, 27, 12 (1988) 2549–2553.
38. Wan, Y., McIntosh, K. R., and Thomson, A. F., Characterisation and Optimisation of PECVD SiN_x as an Antireflection Coating and Passivation Layer for Silicon Solar Cells, *AIP Advances*, 3, 3 (2013).
39. El Amrani, A., Menous, I., Mahiou, L., Tadjine, R., Touati, A., and Lefgoum, A., Silicon Nitride Film for Solar Cells, *Renewable Energy*, 33, 10 (2008) 2289–2293.
40. Liu, B., Zhong, S., Liu, J., Xia, Y., and Li, C., Silicon Nitride Film by Inline PECVD for Black Silicon Solar Cells, *International Journal of Photoenergy*, 2012, (2012) 2–7.
41. Lipiński, M., Silicon Nitride for Photovoltaic Application, *Archives of Material Science and Engineering*, 46, 2 (2010) 69–87.
42. Macleod, A., *Thin-Film Optical Filters*, Fourth Edi. CRC Press, 2010.
43. Dobrowolski, J. A., Optical Properties of Films and Coatings, in *Handbook of Optics: Volume IV - Optical Properties of Materials, Nonlinear Optics, Quantum Optics*, McGraw-Hill Professional, 2010.

44. Doyle, W. T., Graphical Approach to Fresnel's Equations for Reflection and Refraction of Light, *American Journal of Physics*, 8. 48 (1980) 643-647.
45. Fresnel's Equation For Reflection and Transmission.
https://www.brown.edu/research/labs/mittleman/sites/brown.edu.research.labs.mittleman/files/uploads/lecture13_0.pdf. 28 Nov 2018.
46. Honsberg, C., and Bowden, S., Optical Losses.
<https://www.pveducation.org/pvcdrom/optical-losses>. 28 Nov 2018.
47. Sardarzaei, A., and Kiamehr, Z., The Optical Constants Determination of Thin-Films, *Cumhuriyet University Faculty of Science Journal*, 46, 3 (2015).
48. Uzum, A. et al., Sprayed and Spin-Coated Multilayer Antireflection Coating Films for Nonvacuum Processed Crystalline Silicon Solar Cells, *International Journal of Photoenergy*, 2017.
49. Bouhaf, D., Moussi, A., Chikouche, A., and Ruiz, J. M., Design and Simulation of Antireflection Coating for Application to Silicon Solar Cells, *Solar Energy Materials and Solar Cells*, 73, 52 (1998) 79-93.
50. Heavens, S., *Optical Properties of Thin Solid Films*, 2nd edition. Dover Publications, 2011.
51. Katsidis, C. C., and Siapkias, D. I., General Transfer-Matrix Method for Optical Multilayer Systems with Coherent, Partially Coherent, and Incoherent Interference, *Applied Optics*, 41, 19 (2002) 3978-3987.
52. Lecaruyer, P. et al., Generalization of The Rouard Method to an Absorbing Thin Film Stack and Application to Surface Plasmon Resonance, *Applied Optics*, 45, 33 (2006) 8419-8423.
53. Rodríguez-de Marcos, L. V., Larruquert, J. I., Méndez, J. A., and Aznárez, J. A., Self-Consistent Optical Constants of SiO₂ and Ta₂O₅ Films, *Optical Materials Express*, 6, 11 (2016) 3622-3637.
54. Polyanskiy, M. N., *Refractive Index Info Database*.
<https://refractiveindex.info/cite.php>. 22 Nov 2018.
55. *Refractive Index Library*. [https://www2.pvlighthouse.com.au/resources/photovoltaicmaterials/refractive index/refractive index.aspx](https://www2.pvlighthouse.com.au/resources/photovoltaicmaterials/refractive%20index/refractive%20index.aspx). 22 Nov 2018.

56. Yang, Z.-P., Cheng, H.-E., Chang, I.-H., and Yu, I.-S., Atomic Layer Deposition TiO₂ Films and TiO₂/SiN_x Stacks Applied for Silicon Solar Cells, *Applied Sciences*, 6, 8 (2016) 233-244.
57. Cid, M., Stem, N., Brunetti, C., Beloto, A. F., and Ramos, C. A., Improvements in Anti-Reflection Coatings for High-Efficiency Silicon Solar Cells, *Surface and Coatings Technology*, 106, 2-3 (1998) 117-120.
58. Clugston, D. A., and Basore, P. A., PC1D Version 5- 32-Bit Solar Cell Modeling on Personal Computers, 26th IEEE Photovoltaics Specialist Conference, October 1997, Anaheim California, 207-210.
59. Green, M. A., Depletion Region Recombination in Silicon Thin-Film Multilayer Solar Cells, *Progress in Photovoltaics*, 4, 5 (1996) 375-380.
60. Hurkx, G. A., Klaasen, D. B., and Knuvers, M. P., A New Recombination Model For Device Simulation Including Tunneling, *IEEE Transactions on Electron Devices*, 39, 2 (1992) 331-338.

CURRICULUM VITAE

Born on 03.08.1990 at Cotabato City, Philippines. Finished Bachelor of Electronics and Communications Engineering at Notre Dame University, Cotabato City, Philippines. Attended various Programming and IT-Based trainings (Microsoft, EMC², Programming, Networking, Troubleshooting). Passed the licensure examination for Electronics Engineers at Professional Regulations Commissions, Philippines. Became an Instructor at AMA Computer College, Cotabato City and technical instructor at Technical Education and Skills Development Authority, Philippines. Started studying as a government scholar (Turkey Scholarships) on Electrical and Electronics Engineering at Karadeniz Technical University on 2016. Awarded ERASMUS+ scholarship for 1 semester on 2017 at Universitat Kassel, Germany. Can write and speak technical English fluently and have proficiency of Turkish.